NAVAL FACILITIES ENGINEERING SERVICE CENTER
Port Hueneme, California 93043-4370

Technical Report
TR-6056-OCN

MOORING LOADS DUE TO PARALLEL PASSING SHIPS

by

David Kriebel, P.E., Ph.D.
Ocean Engineering Program
United States Naval Academy
Annapolis, MD 21402

30 September 2005

Supported by:

William Seelig, PE
Naval Facilities Engineering Service Center
720 Kennon Street SE Suite 333
Washington, DC 20374

Martin Eskijian, PE
Marine Facilities Division California
State Lands Commission 200
Oceangate, Suite 900
Long Beach, CA 90802

Prepared for:

Commander, Naval Facilities Engineering Command
Engineering Innovation & Criteria Office

EXECUTIVE SUMMARY

If a moving ship passes close to a moored ship, hydrodynamic loads are imparted on the moored ship. These loads must be resisted by the mooring system and include time varying surge and sway forces, as well as time-varying yaw moments.

In this study, laboratory scale model tests were conducted to measure the loads on a moored ship resulting from a passing ship moving parallel to the moored vessel. Variations in the model tests included changes in the passing vessel speed, vessel displacement, water depth, and separation distance between the two ships.

The laboratory data have been analyzed in several ways. First, empirical equations were developed that describe the variation in the peak mooring loads with changes in the above parameters. These equations notably describe the increase in loads with the increasing speed of the passing vessel, the increase in loads with increasing draft-to-depth ratio, and the decrease in loads with increasing separation between the vessels.

Second, two existing predictive models were evaluated in “blind” tests to determine their ability to predict the measured mooring loads. One method, developed by Flory (2002), generally under-predicted surge and sway forces, but was found to be inconsistent in the way that it includes variable displacement of the passing ship and in the way that it accounts for changing water depth. A second method, the PASS-MOOR spreadsheet of Seelig (2001) also under-predicted the measured loads but did so in a consistent way. As a result, empirical correction factors were developed for use with PASS-MOOR that improve its predictive capability.

INTRODUCTION

A series of scale model tests were performed to document the hydrodynamic loads on a moored ship due to a passing vessel. These loads include the surge force, sway force, and yaw moment experienced by the moored vessel, for the case where the moored ship is parallel to the passing ship.

The primary goals of this work are: (1) to expand the experimental database for mooring loads generated by passing ships and (2) to refine simplified predictive methods based on the new laboratory data. In this work, two predictive models are evaluated using the new experimental data. One method, by Flory (2002), consists of empirical equations for the mooring forces and yaw moments. The other method, by Seelig (2001), consists of an Excel spreadsheet, PASS-MOOR, which implements a hydrodynamic interaction theory by Wang (1975) along with empirical modifications. In addition to these models, a new empirical model is developed based on the lab data.

BACKGROUND

It is well-known that if a moving ship passes close to a moored ship, hydrodynamic interactions between the two vessels cause surge and sway forces, as well as yaw moments, on the moored vessel, e.g. Remery (1974), Muga and Fang (1975), Wang (1975), and others. If the passing vessel is moving at high speed, if the separation distance between the vessels is small, and/or if the vessels have minimal underkeel clearance, the mooring loads can be quite large. In fact, there are numerous documents cases of serious accidents resulting from this interaction. One such case is the fire and explosion of the tanker JUPITER caused by a passing vessel as documented, along with other cases, in Seelig (2001).

At present, there are few validated methods of predicting the hydrodynamic interaction and resulting loads on the moored vessel. Predictive methods generally fall into one of two general types: (1) time-stepping numerical models that simulate the fluid velocities and pressures forces due to a moving ship and then integrate pressures around the moored ship to determine loads or (2) simplified engineering methods that provide a direct estimate of forces on the moored ship through simple equations and/or design graphs.

The time-stepping models are generally based on either the slender-body approximation of the ship hull, e.g. Wang (1975) or Cohen and Beck (1983), or on more exact panel methods that can represent actual 3-D hull forms, e.g. Korsmeyer et al. (1993) or Pinkster (2004). The newer numerical codes have many advantages in that they can represent any ship hull form, and they can represent such conditions as confined channels and moored ships backed by quay walls. At present, however, none of these computer codes is owned by either sponsors of this study, NAVFAC or the California State Lands Commission.

The second type of predictive method, empirical equations or simplified spreadsheets, are presently used within both NAVFAC and the California State Lands Commission and are therefore the focus of the present study. As noted, two simplified predictive methods are presently available. One method, developed by Seelig (2001), is a spreadsheet called PASS-MOOR that is based on theoretical predictions of Wang (1975). Wang's method gives mooring loads for deep water where the vessel draft is small compared to the water depth. Seelig then modified Wang's theoretical solution by including empirical correction factors to account for finite depth (small underkeel clearance). These correction factors were based on analysis of laboratory test data as reported by Remery (1974) and Muga and Fang (1975). The second predictive method, developed by Flory (2002), consists of empirical equations for surge force, sway force, and yaw moment. These were derived from the Remery (1974) data, which are applicable in shallow water. Flory then developed correction factors for other values of underkeel clearance based on the test data of Muga and Fang (1975).

As the preceding paragraph indicates, both of the simplified prediction methods use empirical results from the same limited laboratory tests conducted by Remery (1974) and Muga and Fang (1975). Interestingly, both sets of data were obtained from the same laboratory facility, the Netherlands Ship Model Basin, and both used similar scaled models of large oil tankers. Given the limited number of tests performed, and the fact that both predictive methods have an empirical basis in the same data sets, it is not clear how well these methods apply outside of the range of conditions tested.

DESCRIPTION OF PROJECT

The present study addresses these issues through additional scale model tests, through analysis of the existing predictive methods to assess their validity in predicting the measured mooring loads, and through development of new empirical equations to predict mooring loads.

The first goal of this study was to expand the database for mooring loads caused by passing ships, and 144 model tests were then carried out at the U.S. Naval Academy. These tests were conducted using generic "Series 60" hull forms representative of commercial vessels with high block coefficients. Tests were conducted for the case in which the passing ship travels in a direction parallel to the moored ship. Variables in the test plan then included the passing ship draft, the water depth, the passing ship speed, and the separation distance between the ships. Measurements included the time-histories of the surge force, sway force, and yaw moment. Peak values of all three parameters were then extracted for further analysis.

The second goal of this study was to develop a set of empirical equations for the peak surge force, sway force, and yaw moment from the new data. These equations are in some ways similar to those developed by Flory (2002) but are based on the new model data rather than on the earlier test data of Remery (1974). These equations are given in dimensionless form and allow prediction of the maximum force and moments based on basic parameters such as the draft-to-depth ratio, the relative separation

distance (normalized by ship length), and the displacement ratio defining the size difference between the passing and moored ships.

The third goal of this study is the validation and verification of the two existing predictive methods of Flory (2002) and Seelig (2001). Both methods were applied "blindly" to the new lab data in order to determine their ability to predict measured mooring loads without further adjustment in their empirical coefficient.

A follow-on part of this analysis involved development of new empirical coefficients for use in the Seelig method. As noted, Seelig's spreadsheet PASS-MOOR combines the theory of Wang (1975) for deep water with empirical correction factors for finite depth developed from the lab data of Remery (1974) and Muga and Fang (1975). In order to preserve use of the underlying theory of Wang, but improve the ability of PASS-MOOR to predict measured mooring loads, new empirical correction factors were developed to account for reduced underkeel clearance.

DESCRIPTION OF EXPERIMENTS

Test Configuration

All tests conducted in this study use the parallel configuration indicated in Figure 1 (a), in which the passing ships moves parallel to, and in the same direction as, the moored ship. Model tests were later conducted using the perpendicular configuration shown in Figure 1(b) but these results are presented in a separate data report.

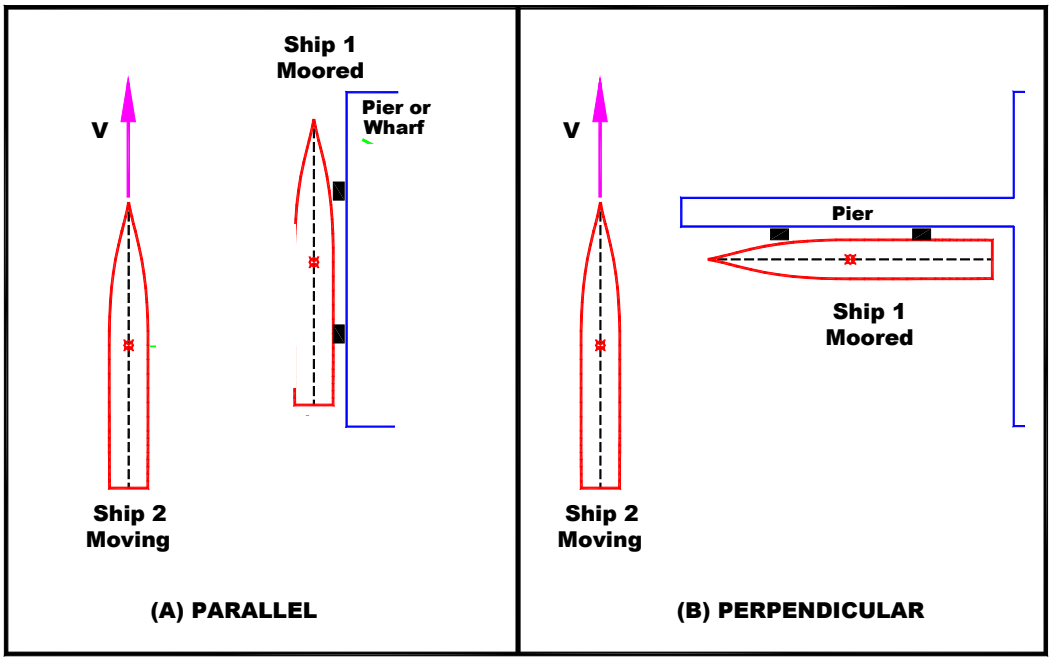

Figure 1. Model test configurations

Facility and Test Rigs

The study required testing in shallow water in a wide towing tank, in order to minimize side wall effects. The existing towing tanks at the Naval Academy were too narrow or could not be used with shallow water depths, so tests were conducted in the wider Coastal Engineering basin instead. The tests section of the coastal engineering basin is rectangular, and is 40 ft long and 18 ft wide. Water depths are adjustable and ranged from 4.1 inches to 14.5 inches.

The tank did not have towing capability, so a new towing system was designed and constructed for this project. The towing rig consisted of an aluminum frame that spanned the entire 40 ft length of the basin, a closed-loop cable drive system, a towing carriage (attached to the drive cable) that rolled along the frame, and a variable speed drive motor. The "passing ship" model was attached under the towing carriage by means of a heave post and pitch pivot that allowed the model to move vertically as the water level was changed from run to run and to achieve realistic squat and trim during model tests. Figure 2 gives an overview of the towing rig in the basin while Figures 3a and 3b show views of the towing carriage with the passing ship attached.

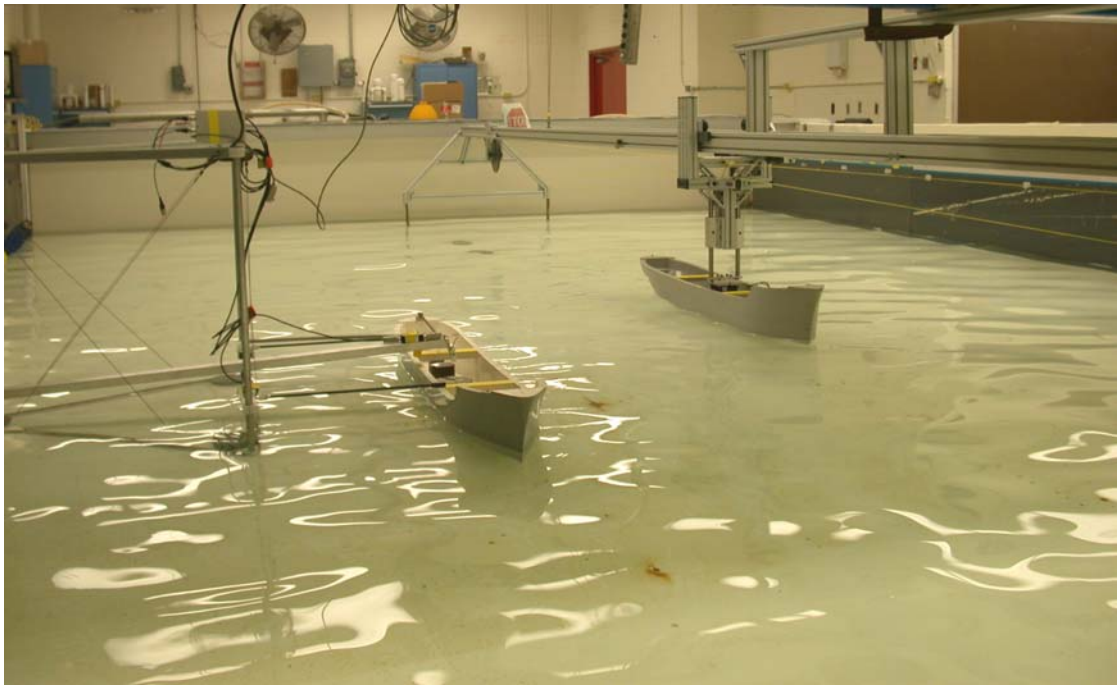

Figure 2. View of Coastal Engineering Basin with moored ship in foreground and passing ship in background. Passing ship is attached to towing carriage that rolls along aluminum frame.

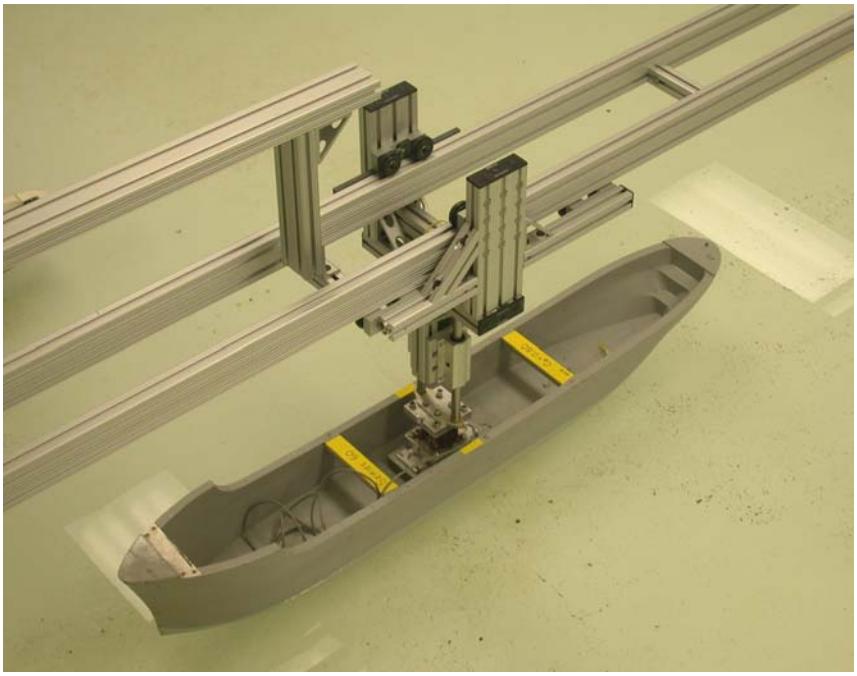

Figure 3a. View of towing carriage on aluminum frame.
Model is driven by thin cable under aluminum frame (not visible in photo).

Figure 3b. View of towing carriage attached to drive cable.

In addition, significant work was required to design and construct a mooring rig that would allow surge and sway forces, as well as yaw moments, to be measured on a moored ship model. This measurement rig was designed and constructed concurrent with the development of the towing rig. In fact, two test rigs were developed.

The first test rig was constructed using a heavy aluminum frame and is shown in Figures 4 and 5. With this rig, square modular force blocks were mounted in the ship model and were attached to the aluminum frame using vertical guide rails running through roller bearings fore and aft. These restrained the model in surge, sway, and yaw while allowing heave and pitch motions. Surge and Sway forces were measured at both the fore and aft gage locations.

While this test rig was used successfully in one test series (tests using one water depth of 4.9 inches), it proved troublesome and was eventually replaced. Problems arose due to occasional binding of the vertical rollers and due to use of the modular force blocks. These force blocks had 5 and 10 pound capacities and had difficulty resolving the small loads being experienced, which were sometimes on the order of 0.01 pounds.

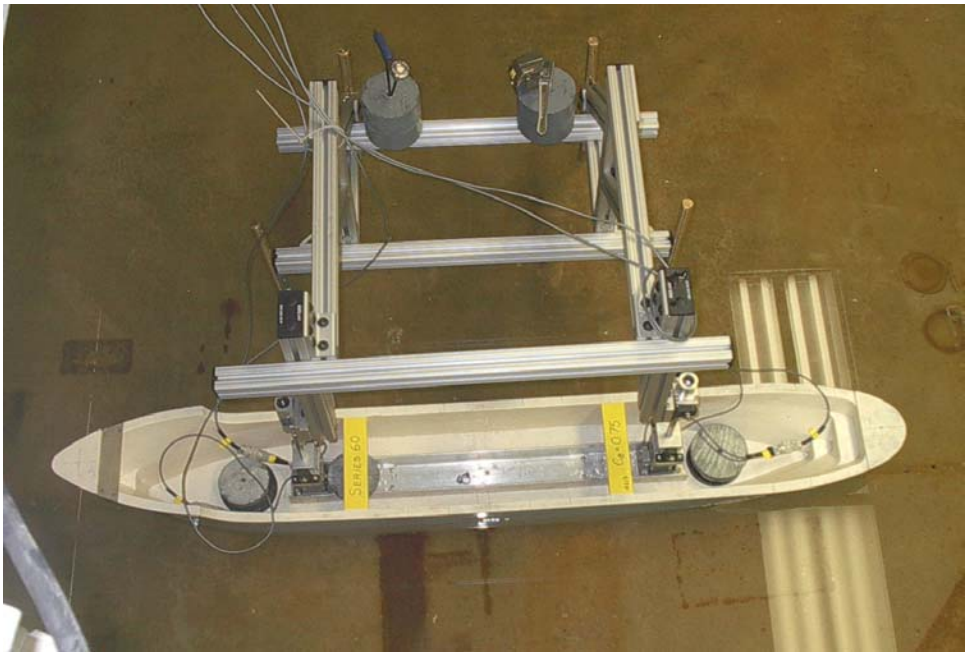

Figure 4. Original test frame used to measure mooring loads, viewed from top

Figure 5. Original test frame used to measure mooring loads, viewed from front

A second test rig was then constructed and was used for the bulk of the laboratory experiments. This rig, shown in Figures 6a and 6b, consisted of a light weight aluminum frame. The moored ship model was attached to the frame using lightweight carbon-fiber rods, with one rod providing restraint in the surge direction and two providing restraint in the sway direction. Universal joints at the ends of each rod allowed the model to move in heave, pitch, and roll modes.

Three load cells were then placed on the aluminum frame and were connected to the carbon fiber rods: one to measure surge force and two (fore and aft) to measure sway force and yaw moment. The force gages were small 2 pound capacity load cells with a resolution of about 0.005 pounds. A close-up view of the load cell used to measure the surge force is shown in Figure 7.

Measurements were also made of the passing ship speed and position as a function of time. Two electronic switches were located along the aluminum frame supporting the towing rig. These switches were located 15 feet apart and were located at a known location relative to the center of the moored ship. Ship speed could be determined from the time it took the passing ship to move from one switch to the other. The location was then scaled based on the distance from the first switch to the moored ship.

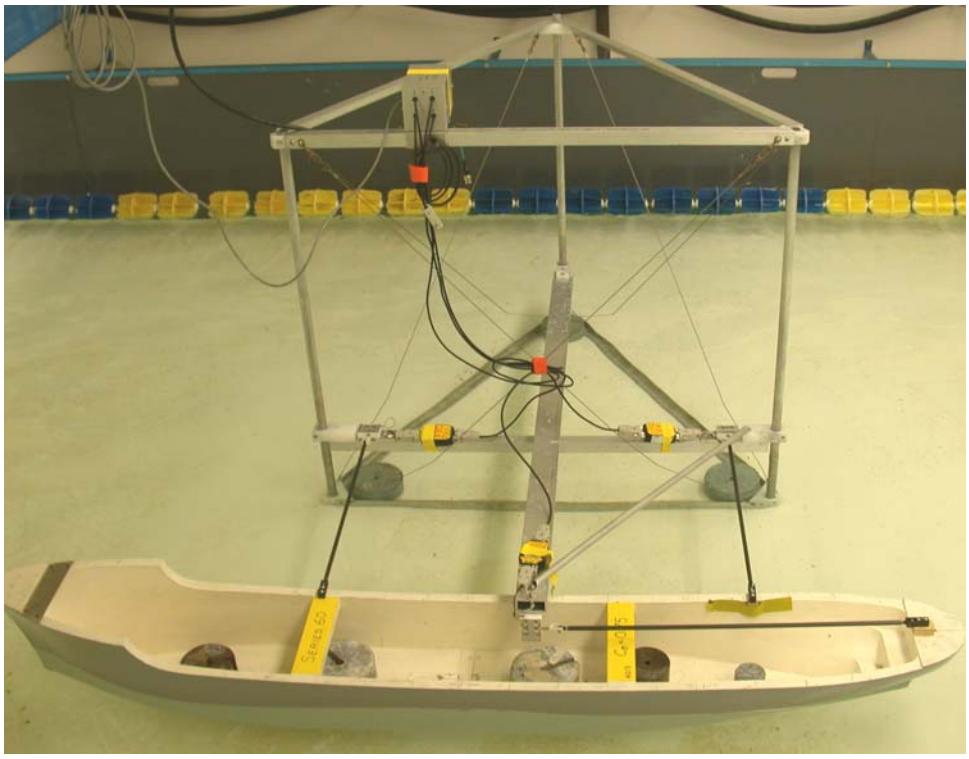

Figure 6a. Final test rig used to measuring mooring loads, viewed from side.

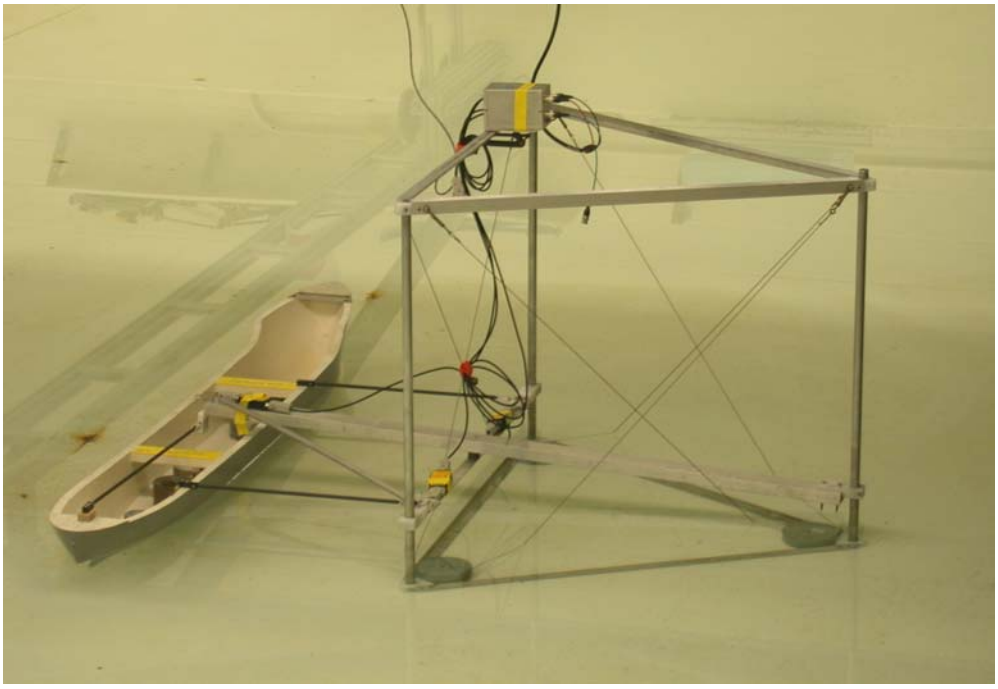

Figure 6b. Final test rig used to measuring mooring loads, viewed from back.

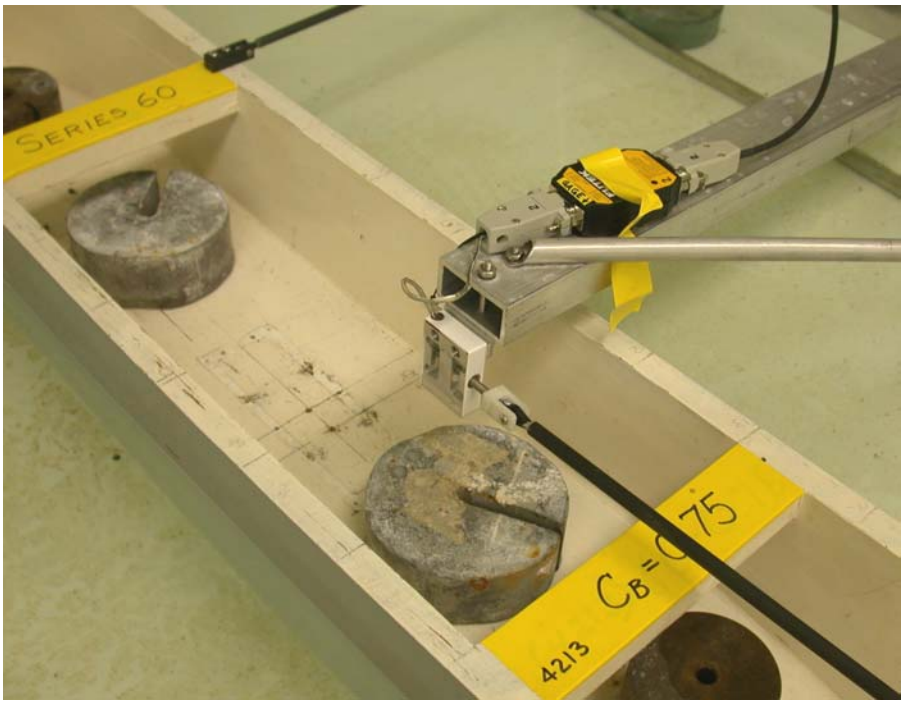

Figure 7. View of load cell used to measure mooring loads.

Ship Models

Two ship models were used in the tests. Both are part of the “Series 60” model series used widely in naval architecture laboratories world wide. These are generic hull forms and are not scaled replicas of any particular full-scale ship.

The two models have the same length, L = 5 ft, but have different beams, drafts, and block coefficients. Detailed parameters are given in Table 1. All tests were performed with the same moored ship having a beam B = 8.9 inches, draft D = 3.7 inches, displacement Δ = 51.6 lbs, and block coefficient C_B = 0.75. All tests used the same passing ship with B = 9.2 inches, but the draft was varied between a “deep draft” and a “shallow draft” condition. The deep draft condition, used in most of the lab tests, had D = 3.7 inches, Δ = 59.0 lbs, and C_B = 0.8. The shallow draft condition then had D = 1.75 inches and Δ = 27.9 lbs.

Photographs of the Series 60 models are given in Figure 8. Figure 8a (top) shows a side view of the larger model (passing vessel). Figure 8b (bottom) shows a top view of the smaller vessel (moored vessel). In this view, the waterline shape is evident and it is noted that the Series 60 models have a nearly symmetric waterline shape bow to stern.

Table 1. Parameters for ship models

Parameter	Moored Ship	Passing Ship	
		Deep Draft	Shallow Draft
L = length	5 ft	5 ft	5 ft
B = Beam	8.9 in	9.2 in	9.2 in
D = Draft	3.7 in	3.7 in	1.75 in
Δ = Displacement	51.6 lbs	59.0 lbs	27.9 lbs
CB = Block Coef	0.75	0.8	0.8

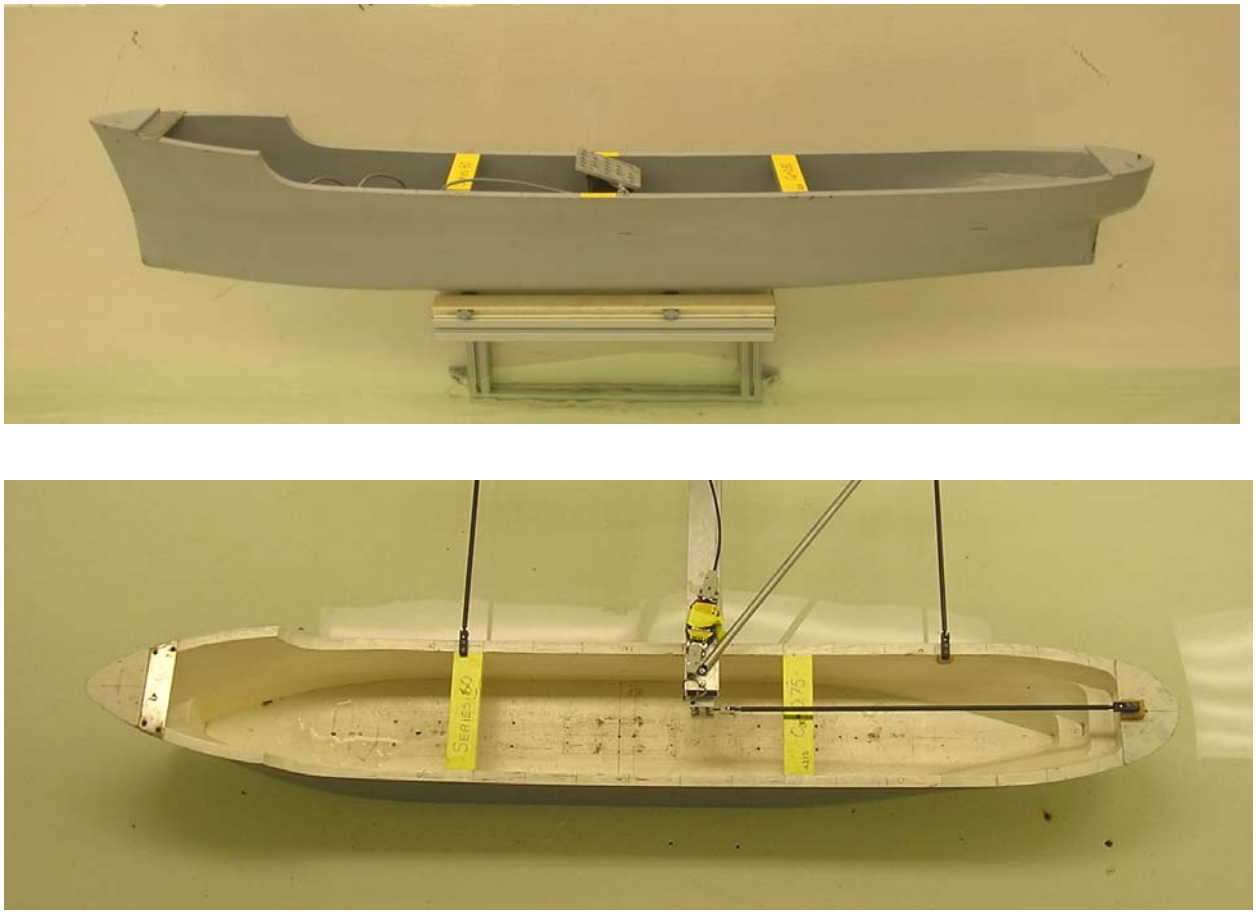

Figure 8. Photographs of Series 60 Models

Test Conditions

Test conditions are listed in Tables 2, 3, and 4. Table 2 gives test conditions in model-scale units. Table 3 then gives comparable test conditions for an assumed full-scale ship. While model test results may, in principle, be scaled up to any full-scale ship size, values in Table 3 give an indication of values for a PANAMAX-size vessel where the beam is limited to 104 feet.

Values listed in Table 2 are exact except for the passing ship speeds. The variable-speed drive motor used on the towing carriage required a manual adjustment of the speed setting that could not be precisely duplicated for each test. As a result, speeds listed in Table 2 are target values; actual speeds were determined from the voltage records of the two electronic switches located 15 ft apart on the towing rig.

Table 2. Range of model test parameters.

	Model Scale
Passing Ship Draft	D = 3.7 in, 1.75 in
Water Depth	d = 4.1, 4.5, 4.9, 5.5, 8.4, and 14.5 inches
Passing Ship Speeds	V = 0.8, 1.0, 1.3, 1.5, 1.8, and 2.0 ft/sec
Separation Distances	S = 1.5, 2, 3, 4, and 5 ft

Table 3. Range of test parameters scaled up to full-scale ship 675 ft long with 104 ft beam.

	Full Scale Assuming Ship Dimensions L = 675 ft B = 104 ft
Passing Ship Draft	D = 41.6 ft, 19.7 ft
Water Depth	d = 46, 51, 55, 62, 95, 163 ft
Passing Ship Speeds	V = 5.5, 6.9, 8.9, 10.3, 12.4, 13.8 knots
Separation Distances	S = 202, 270, 405, 540, and 675 ft

Table 4 then gives test conditions in dimensionless form. Three key dimensionless parameters are:

- **Draft-to-Depth Ratio, D/d** - defined as the draft of the moored ship relative to the water depth
- **Separation Ratio, S/L** - defined as the centerline-to-centerline separation distance relative to moored ship length
- **Displacement Ratio, Δ_R** - defined as the displacement of the passing vessel relative to that of the moored vessel.

Water depths in the model tests were selected to produce a range of draft-to-depth ratios from about 0.24 to 0.9. The low end of the range was in relatively deep water with little bottom interaction while the upper range was intended to be more realistic for ships in dredged channels where the draft nearly equals the water depth. The upper limit also corresponded closely with the Remery (1974) tests.

Separation ratios ranged from 0.3 to 1.0. The low end of the range had ship models very close together with a gap between the outside of the hulls being about equal to the beam of the moored ship. The upper end of the range was effectively the largest separation possible in the coastal engineering basin. For S/L=1, the moored ship was closer to the side wall of the basin than to the passing ship.

Displacement ratios included just two values. When the passing vessel was in the “deep draft” configuration, the displacement was 1.10 times that of the moored vessel. The displacement was then 0.50 times that of the moored vessel when the passing ship was at “shallow draft.”

Table 4. Dimensionless parameters for test conditions

Draft -to-Depth Ratio	D/d = 0.90, 0.82, 0.74, 0.67, 0.43, and 0.25
Separation Ratio	S/L = 0.3, 0.4, 0.6, 0.8, and 1.0
Displacement Ratio	Δ_R = 1.10, 0.52

Not all possible combinations of conditions shown in the above tables were actually tested. Altogether, 144 tests were conducted using combinations of the above parameters. These test conditions are listed in Appendix A, along with summary data for the positive and negative maxima of surge force, sway force, and yaw moment as will be discussed below.

Sign Convention

The coordinate system adopted for tests assumed that the origin (x=0, y=0) was located at midships on the moored ship. The sign convention then follows the "right hand rule" with +X toward the bow, +Y toward port, and the +M counterclockwise, as shown in Figure 9.

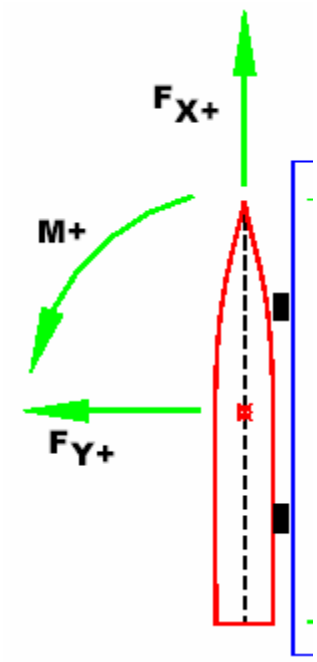

Figure 9. Coordinate system used in tests

Voltage signals from all gages were converted to engineering units in the data acquisition software based on gage calibrations. All forces were measured in units of pounds. Forces measured by the two sway force gages (one near bow, one near stern) were added to obtain the total lateral or sway force. Yaw moments about midships were obtained by multiplying each sway force gages signal by the distance from the gage to midships. Longitudinal or surge forces were obtained from a single force gage in most tests, but were obtained using two force gages for those tests that used the original moored ship test rig.

DATA ANALYSIS

Figure 10 shows a sample time series from the tests, and illustrates basic features of the data analysis. In this graph, the horizontal axis is scaled to represent a dimensionless overtaking distance given as the longitudinal distance between the midships coordinates of the two models, i.e. at x/L=0 the two models are abreast of one another. Negative values of x/L indicate the approach of the passing vessel, while positive values indicate distance as the passing vessel moves past the moored vessel.

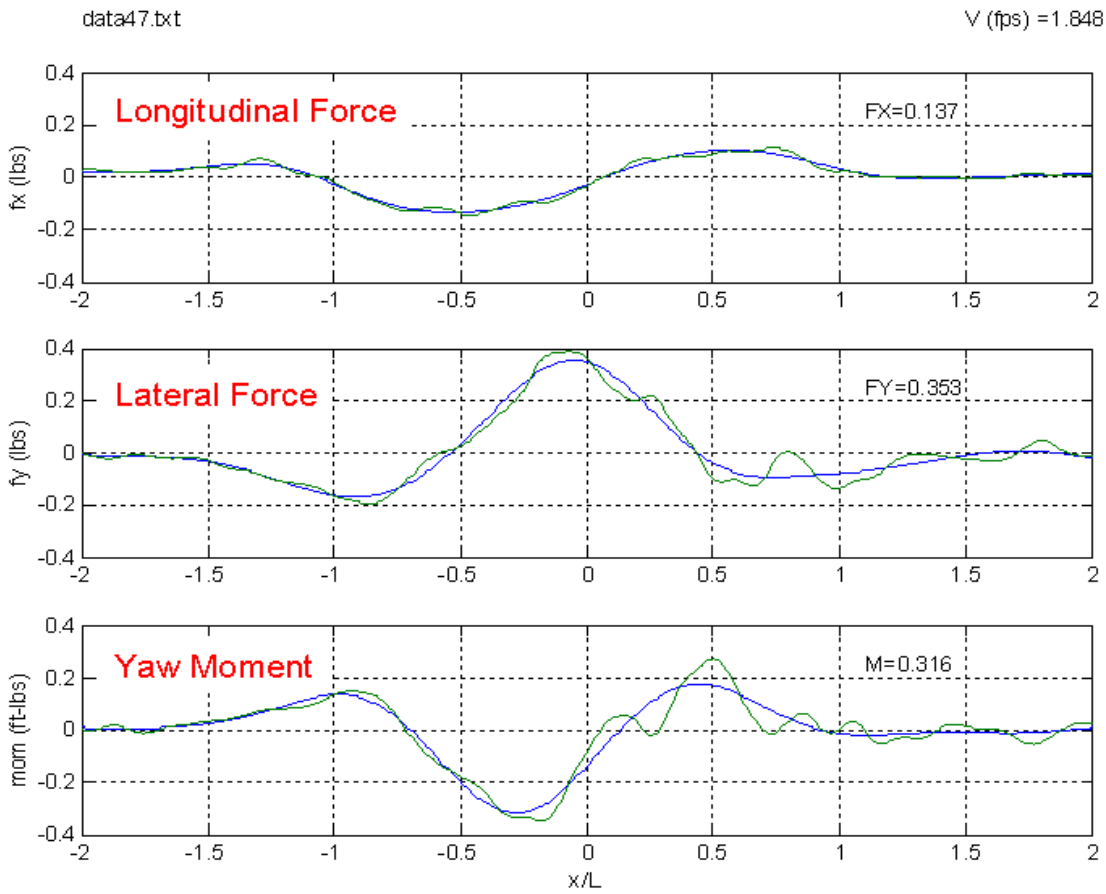

Figure 10. Sample data showing typical measured force and moment records along with low pass filtering.

One feature shown in Figure 10 is the filtering of the raw data to remove various high frequency oscillations. The interest in these tests is in the effects of the primary pressure field which produces low frequency loads on the moored ship. Measurements, however, also included effects of the secondary waves (diverging and transverse ship-generated waves). These were not too evident at the slowest speed tested but became increasingly evident at higher speeds.

In addition, the moored ship exhibited motions at frequencies corresponding to its natural frequencies in surge and sway. Tests were conducted to determine these natural frequencies and it was found that the surge frequency was 3.2 Hz while the sway frequency was about 6 Hz.

In order to remove these higher frequency effects, the raw data was filtered using a low-pass filter with a 2 Hz cutoff frequency. As shown in Figure 10, this effectively removed the high-frequency loads and isolated the low frequency loads of interest. Similar filtering was done by Remery (1974), although it appears that the filtering was done by simply hand-smoothing the data.

Interpretation of Figure 10 is aided by Figure 11 which shows the direction of forces and moments for conditions of a negative overtaking distance (left), ships abreast (center), and a positive overtaking distance (right). The left figure occurs, for example, when X/L = -0.3. As the passing ship approaches, the moored ship experiences a negative surge force, a positive sway force, and a negative yaw moment. When the two ships are abreast, surge forces and yaw moments are near zero, while sway forces are strongly positive, i.e. the moored ship is pulled in toward the passing ship. As the ships part, for example when X/L = +0.6, surge force switch to positive, sway forces switch to negative, and yaw moment switch to positive.

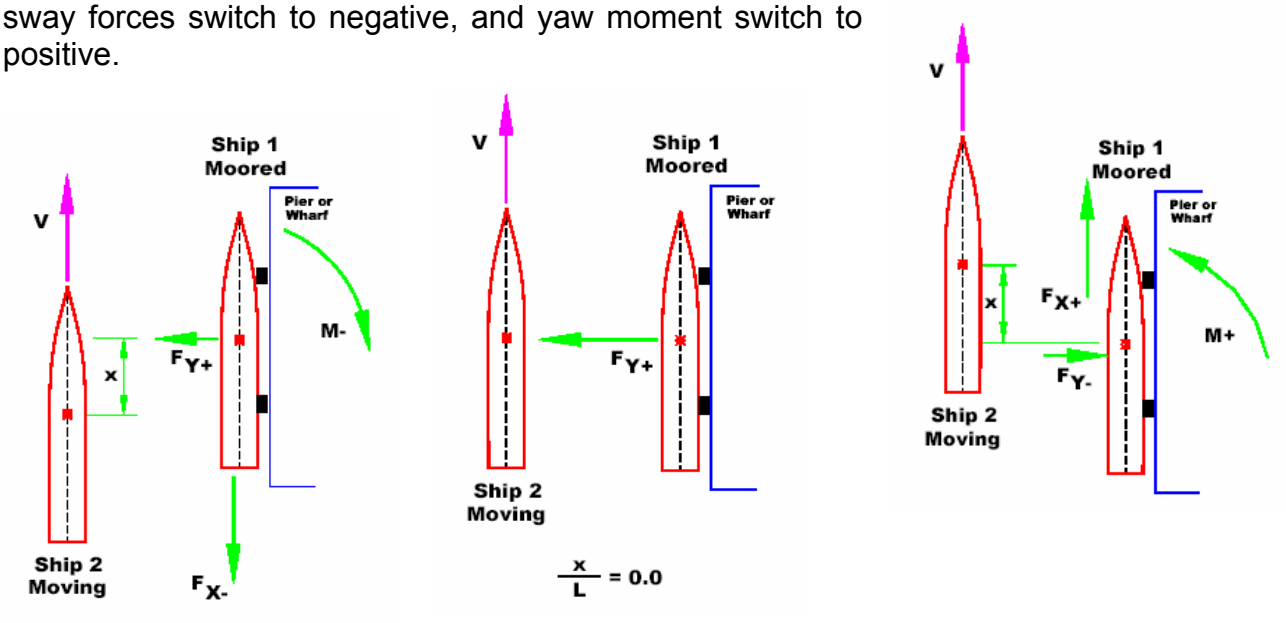

Figure 11. General behavior of loads as vessel approaches (left), passes abeam (center), and departs (right), from Seelig et al (2002).

An idealized description of these loads as a function of X/L is given in Figure 12, which is obtained from Seelig's PASS-MOOR spreadsheet based on Wang's (1975) solution. Loads are given in dimensionless form, normalized by the maximum value.

A comparison of the idealized loads in Figure 12 to the sample loads in Figure 10 shows that measured values have similar dependencies on x/L. But most measurements, like those in Figure 10, do show some variations from the theoretical predictions. In general, while theory suggests that surge force and yaw moment have equal maxima in the positive and negative direction, measurements generally show the negative maxima to be slightly larger than the positive maxima.

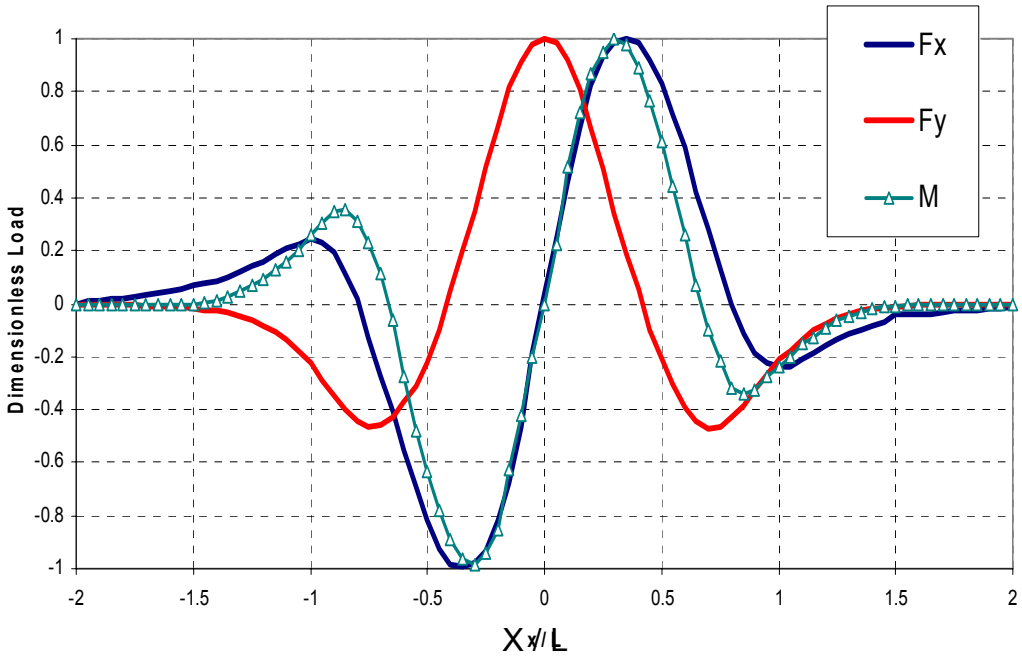

Figure 12. idealized variation of loads with overtaking distance, X/L, based on theory of Wang (1975) as adopted in PASS-MOOR by Seelig et al. (2002).

Repeatability in Tests

Dimensionless plots similar to Figure 10 have been obtained for all data. In some cases, multiple tests were made using the same input condition, i.e. same depth, vessel draft, spacing, and (to within the accuracy possible with the speed control) the same vessel speed. Figure 13 shows an example of the degree of repeatability obtained from five tests of the same condition.

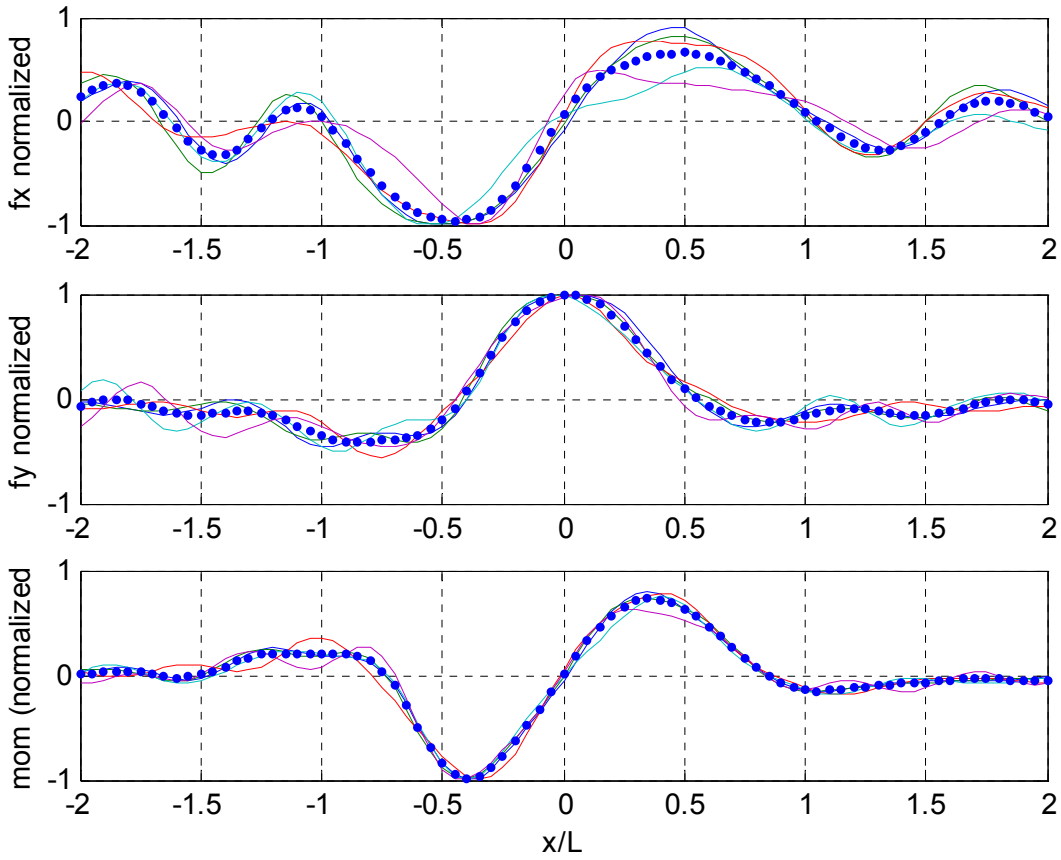

Figure 13. Example of repeatability of 5 tests having the same input conditions. Solid curves represent 5 individual test results. Dotted curve represents average.

Determination of Positive and Negative Maxima

As illustrated in Figure 14, data analysis included a determination of the force and moment maxima in both the positive and negative directions, denoted respectively by “+” and “-“ signs. These are included in Appendix A for all tests.

For the sway force, as noted above, the positive maximum FY+ is without exception larger than the negative maximum FY-. For the surge force, the negative maximum FX- is usually, though not always, larger than the positive maximum FX+. Similar results are found for the yaw moments where M- is usually larger than M+.

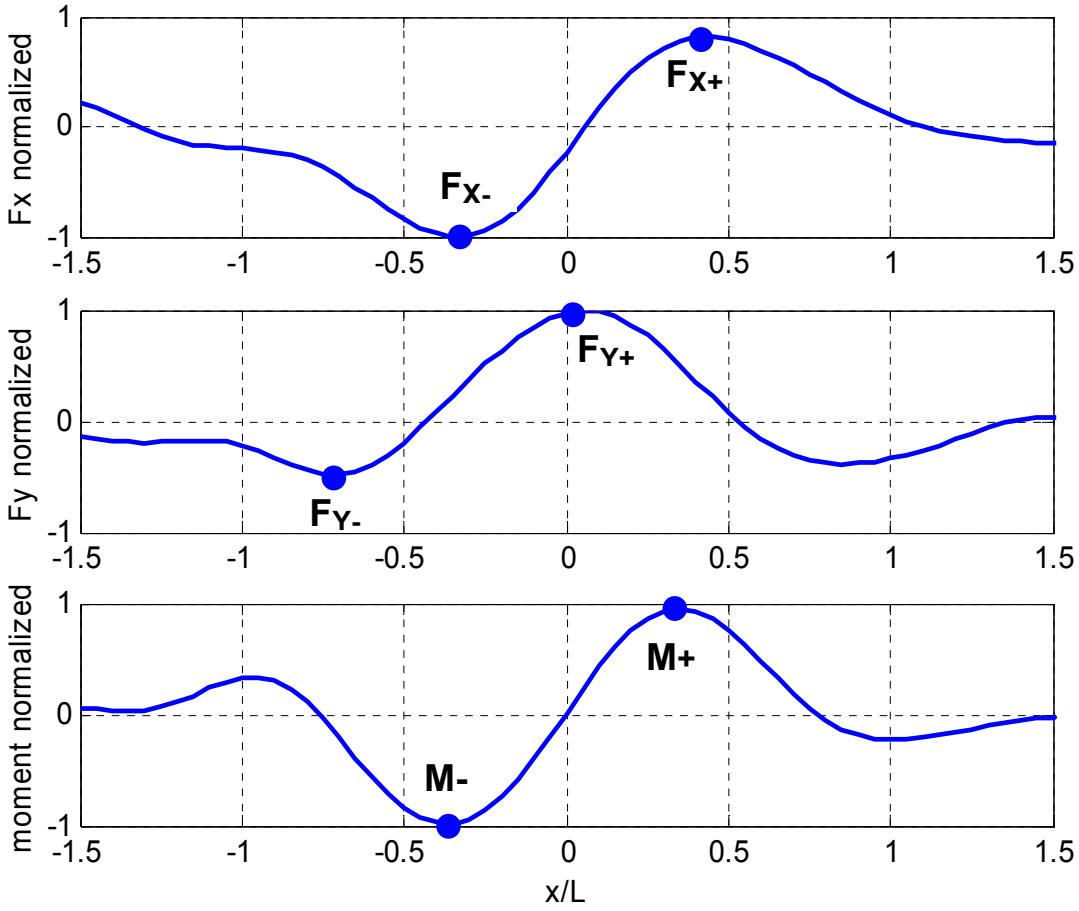

Figure 14. Illustration of positive and negative maxima in forces and moments.

Dimensionless Analysis

One consistent feature of the measured data is that the maximum forces and moments increase with the square of the passing ship speed. This is illustrated in Figure 15 which shows a sample of measured data along with quadratic curves of the form $F \sim V^2$ and $M \sim V^2$.

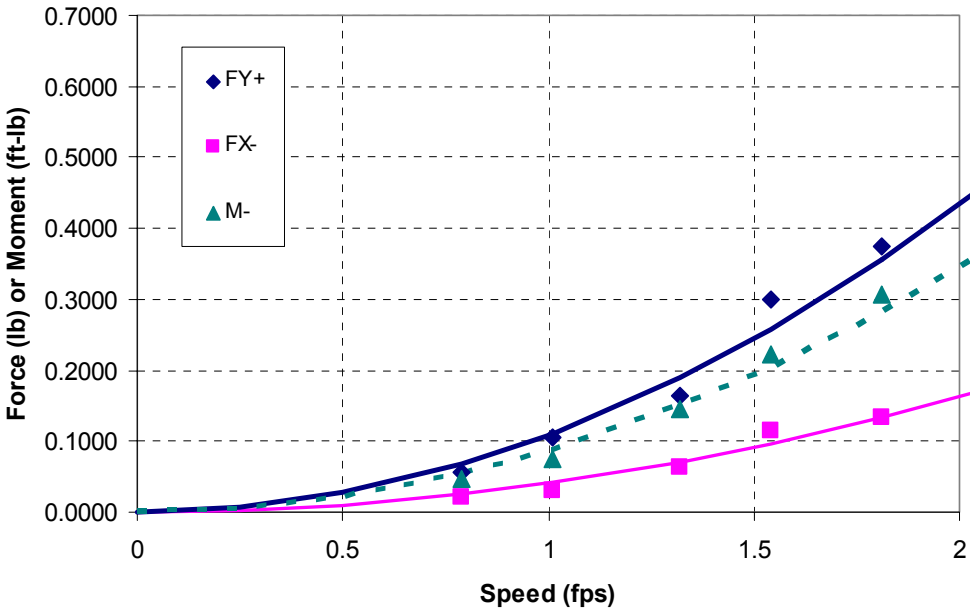

Figure 15. Example showing measured loads varying with square of ship speed, for D=3.7 in, d=4.9 in, and S=2 ft.

As a result, the peak force and moment values can be represented in the following functional form:

$$F_X = C_X \frac{1}{2} \rho D L V^2$$
$$F_Y = C_Y \frac{1}{2} \rho D L V^2 \quad (1)$$
$$M = C_M \frac{1}{2} \rho D L^2 V^2$$

where

ρ	=	Density of water
D	=	Draft of moored ship
L	=	Length of moored ship
V	=	Speed of passing ship
C_X	=	Coefficient for peak surge force
C_Y	=	Coefficient for peak sway force
C_M	=	Coefficient for peak yaw moment

For tests having common values of water depth, passing ship draft, and separation, results for the various passing ship speeds were averaged to define best fit force and moment coefficients. These values are given in Table 5. It is noted that these results are independent of ship speed and depend only on the displacement ratio, Δ_R, the draft-to-depth ratio of the passing ship, D/d, and the separation ratio, S/L.

Table 5
Summary of test results when averaged over all velocities for a given set of test conditions, i.e. for a given ship draft, water depth, and separation.

Passing Draft	Water Depth	spacing	Δ_R	D/d	S/L	CX+	CX-	CY+	CY-	CM+	CM-
inches	inches	feet									
3.7	4.1	2.0	1.1	0.90	0.4	0.0378	0.0463	0.2174	0.1053	0.0274	0.0251
3.7	4.1	3.0	1.1	0.90	0.6	0.0310	0.0306	0.1105	0.0582	0.0133	0.0110
3.7	4.1	4.0	1.1	0.90	0.8	0.0221	0.0239	0.0753	0.0506	0.0073	0.0062
3.7	4.5	2.0	1.1	0.82	0.4	0.0309	0.0369	0.1159	0.0606	0.0129	0.0149
3.7	4.5	3.0	1.1	0.82	0.6	0.0226	0.0268	0.0777	0.0360	0.0069	0.0076
3.7	4.5	4.0	1.1	0.82	0.8	0.0194	0.0240	0.0524	0.0388	0.0039	0.0044
3.7	4.9	1.5	1.1	0.76	0.3	0.0266	0.0353	0.0974	0.0558	0.0110	0.0171
3.7	4.9	2.0	1.1	0.76	0.4	0.0216	0.0270	0.0725	0.0360	0.0082	0.0115
3.7	4.9	3.0	1.1	0.76	0.6	0.0132	0.0190	0.0450	0.0247	0.0044	0.0065
3.7	4.9	4.0	1.1	0.76	0.8	0.0138	0.0171	0.0254	0.0185	0.0025	0.0035
3.7	4.9	5.0	1.1	0.76	1.0	0.0118	0.0164	0.0268	0.0264	0.0028	0.0032
3.7	5.5	2.0	1.1	0.67	0.4	0.0183	0.0227	0.0479	0.0253	0.0051	0.0097
3.7	8.4	2.0	1.1	0.44	0.4	0.0120	0.0150	0.0311	0.0152	0.0048	0.0049
3.7	8.4	3.0	1.1	0.44	0.6	0.0089	0.0089	0.0175	0.0103	0.0025	0.0024
3.7	8.4	4.0	1.1	0.44	0.8	0.0078	0.0087	0.0137	0.0010	0.0013	0.0015
3.7	14.5	2.0	1.1	0.26	0.4	0.0072	0.0082	0.0173	0.0087	0.0027	0.0029
3.7	14.5	3.0	1.1	0.26	0.6	0.0055	0.0058	0.0103	0.0054	0.0013	0.0013
3.7	14.5	4.0	1.1	0.26	0.8	0.0041	0.0043	0.0065	0.0052	0.0007	0.0007
1.75	4.1	2.0	0.52	0.43	0.4	0.0170	0.0185	0.0741	0.0439	0.0102	0.0095
1.75	4.1	3.0	0.52	0.43	0.6	0.0124	0.0156	0.0457	0.0602	0.0044	0.0049
1.75	4.1	4.0	0.52	0.43	0.8	0.0137	0.0146	0.0322	0.0250	0.0031	0.0032
1.75	4.5	2.0	0.52	0.39	0.4	0.0131	0.0159	0.0496	0.0255	0.0063	0.0065
1.75	4.5	3.0	0.52	0.39	0.6	0.0090	0.0124	0.0274	0.0147	0.0031	0.0033
1.75	4.5	4.0	0.52	0.39	0.8	0.0092	0.0115	0.0202	0.0126	0.0017	0.0019
1.75	8.4	2.0	0.52	0.21	0.4	0.0059	0.0064	0.0118	0.0063	0.0022	0.0022
1.75	8.4	3.0	0.52	0.21	0.6	0.0039	0.0044	0.0068	0.0052	0.0011	0.0012
1.75	8.4	4.0	0.52	0.21	0.8	0.0031	0.0033	0.0051	0.0047	0.0006	0.0006

Some results from Table 5 are presented graphically in Figures 16 and 17. These are from tests with largest displacement ratio, Δ_R =1.1.

In Figure 16, the maximum load coefficients (CX-, CY+, and M-) are plotted against the separation ratio, S/L. As expected, results indicate the largest loads for the smallest separation, S/L=0.4, with loads diminishing as S/L increases. Loads are also largest when underkeel clearance is small, i.e. for D/d=0.90, and diminish as D/d decreases. The sway coefficient, CY+, is two to four times larger than the surge force coefficient, CX-.

Figure 17 then shows that same data plotted against the draft-to-depth ratio, D/d. Tests conducted with D/d=0.26 represent the approximate limit of "deep water" with large underkeel clearance. Loads increase dramatically in shallow water approaches unity. For the smallest underkeel clearance tested of D/d=0.90, loads are an order of magnitude larger than the deep water values. Loads increase strongly with increasing D/d, especially for D/d greater than 0.7. Loads also increase most dramatically for the smallest separation ration of S/L=0.4.

EMPIRICAL MODEL

The smooth variations in load coefficients displayed in Figures 16 and 17 suggest that relatively simple empirical formulations may be obtained for these coefficients. In particular, it may be observed in the data that the coefficients: (1) diminish in an exponential fashion with increasing separation ratio, S/L, and (2) increase in an exponential fashion with increasing draft-to-depth ratio, D/d.

Fitting these forms to the data in Table 5 for the peak loads, gives the following relationships:

$$C_{X-} = 0.0074\ \Delta_R\ e^{+2.6(D/d)}\ e^{-1.5(S/L)}$$

$$C_{Y+} = 0.0126\ \Delta_R\ e^{+3.6(D/d)}\ e^{-2.0(S/L)} \qquad (2)$$

$$C_{M-} = 0.0044\ \Delta_R\ e^{+3.2(D/d)}\ e^{-3.4(S/L)}$$

The coefficients in equation (2) are developed for a condition in which the displacement ratio, Δ_R, equals unity, i.e. for a passing ship has a displacement equal to that of the moored ship. Tests were conducted with two values of the displacement ratio and results suggest that the coefficients then vary in approximately a linear fashion with changes in Δ_R. When the passing ship was tested at its largest draft, Δ_R = 1.14, while the passing ship at its smallest draft had Δ_R = 0.52. Load coefficients in Table 5 vary roughly in this proportion (0.52/1.14 = 0.46).

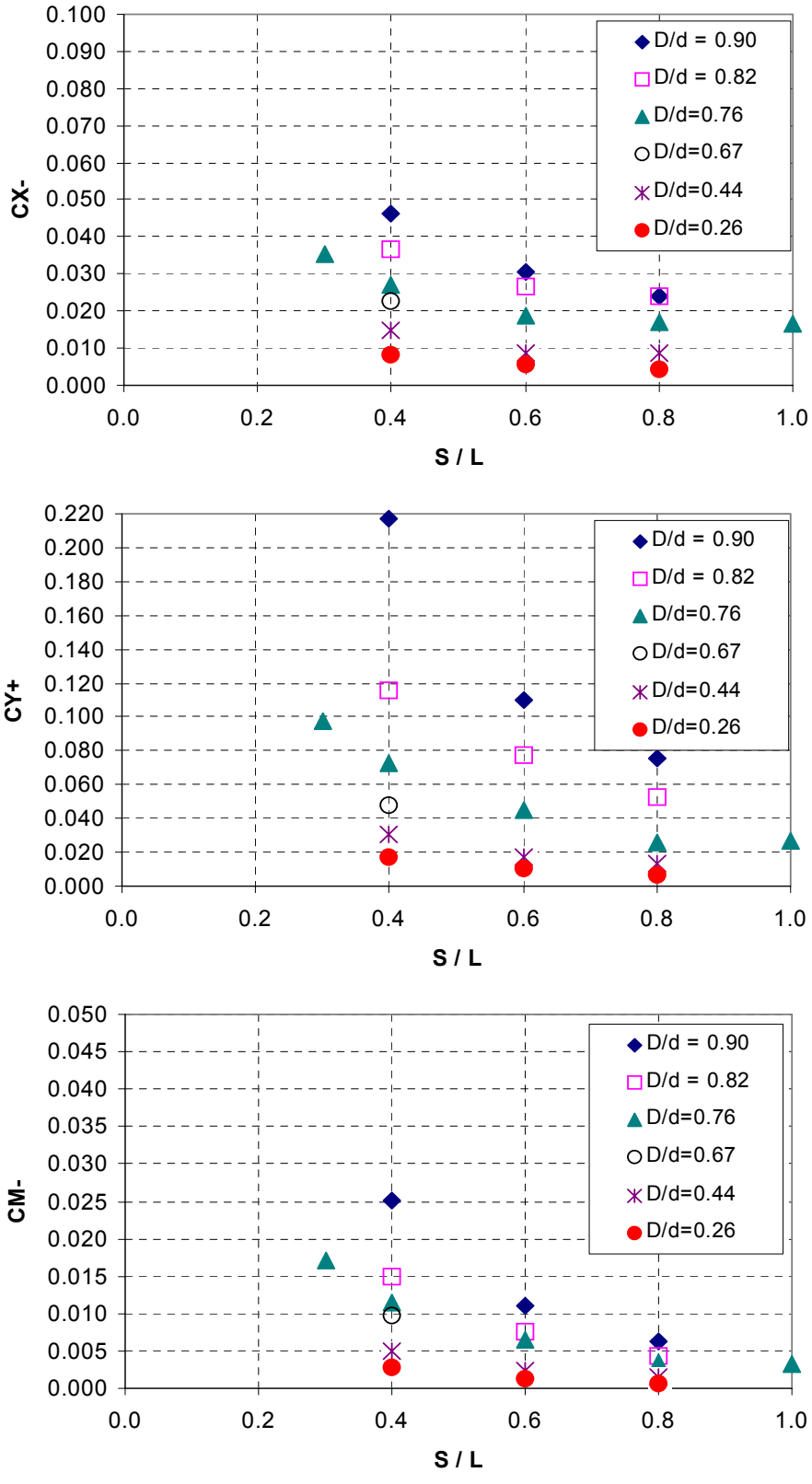

Figure 16. Load coefficients plotted versus separation ratio

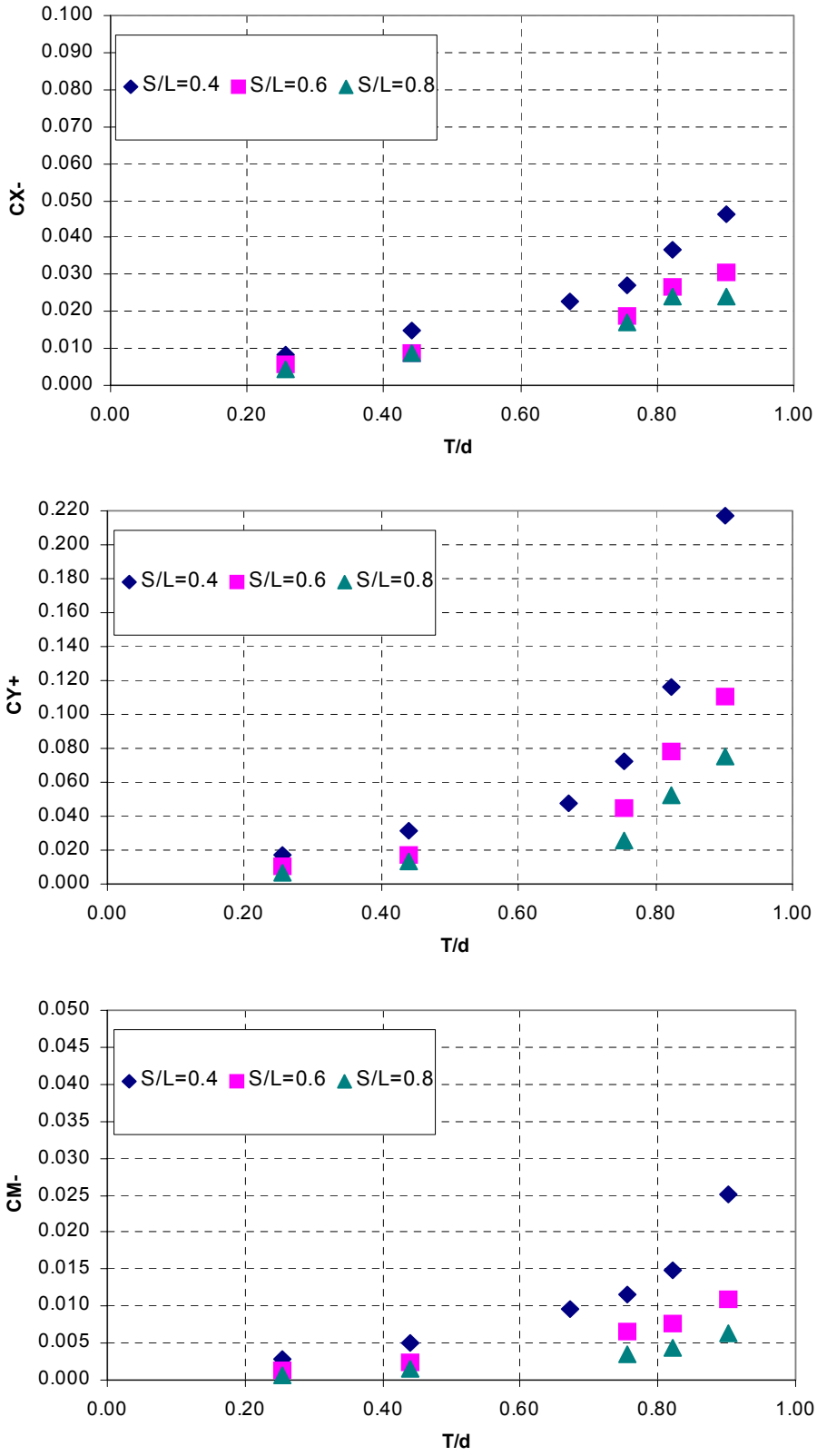

Figure 17. Load coefficients plotted versus draft-to-depth ratio

With the above coefficients, peak loads may be predicted from equation (1) as:

$$F_{X-} = \frac{1}{2}\rho D L V^2 \; C_{X-}$$

$$F_{Y+} = \frac{1}{2}\rho D L V^2 \; C_{Y+} \qquad (3)$$

$$M_{-} = \frac{1}{2}\rho D L^2 V^2 \; C_{M-}$$

As illustrated in Figure 14, these are the peak loads, in the positive direction for F_Y, and in the negative direction for F_X and M. The secondary maxima in the opposite direction can be estimated as

$$X_{+} = 0.85 \quad X_{-}$$

$$Y_{-} = 0.61 \quad Y_{+} \qquad (4)$$

$$M_{+} = 0.91 \; M_{-}$$

These are based on the average relationship between the positive and negative force maxima from the lab tests. As illustrated in Figure 12, the theoretical results of Wang suggest that F_X and M should be larger than indicated with the same magnitude in the positive and negative direction, while the negative sway force should be a little smaller than indicated or about 0.46 F_{Y+}.

Peak loads predicted using equations (2) and (3) have been compared to measured coefficients from Table 5, with results plotted in Figure 18. In each part of the figure, measured and predicted loads are compared to a line of perfect agreement. While the empirical model is developed to give no bias toward over or under predicting the peak loads, some scatter is apparent. This is due to inherent variability in the experiments and due to the simplified nature of the empirical model. Maximum error is on the order of $\pm$ 25% with typical error on the order of $\pm$ 10%. Scatter is largest for the surge force, as this is the smallest load and most difficult to resolve in the measurements.

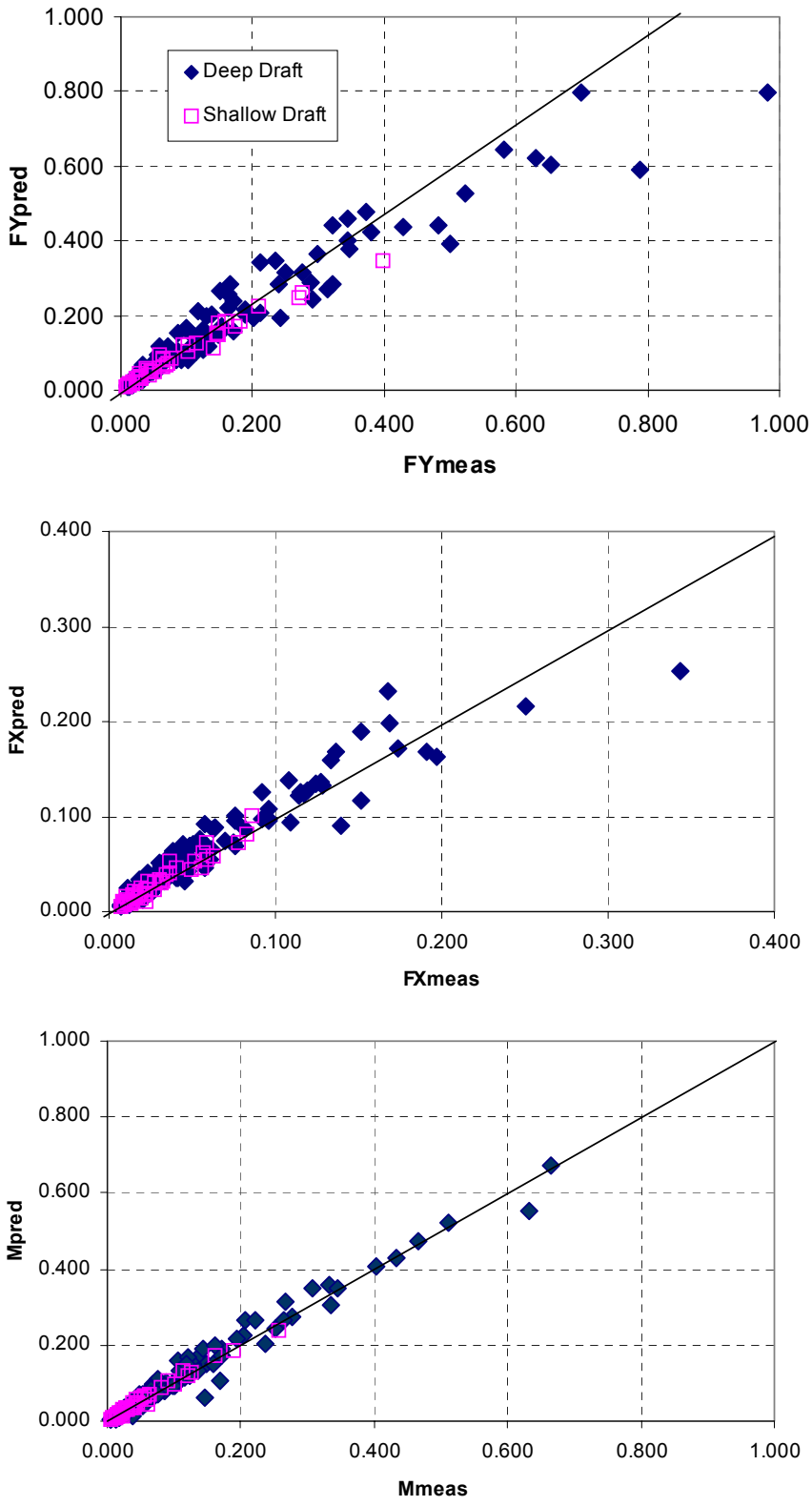

Figure 18. Comparison of measured peak loads to loads predicted using empirical model in equations (2) and (3).

EVALUATION OF PREDICTIVE METHODS

The two existing methods of predicting mooring loads due to passing vessels are now evaluated. These include the empirical equations of Flory (2002) and the empirical corrections to the deep-water theory of Wang used in the PASS-MOOR spreadsheet by Seelig et al. (2002). As noted, both methods are based on scale model tests data of Remery which used models of large oil tankers.

Flory Method

Flory gives the peak loads in the following form:

$$
\begin{aligned}
F_X &= C_X\ S_F\ V^2 \left[0.171 + 0.134\ \ln(\Delta_R) - \left\{ 0.71 + 0.28\ \ln(\Delta_R) \right\} \ln(S_R - 0.06) \right] \\
F_Y &= C_Y\ S_F\ V^2 \left[e^{(1.168\,\Delta_R - 2.25)} - \left\{ 4.41 + 1.93\ \ln(\Delta_R) \right\} \ln(S_R) \right] \\
M &= C_M\ S_M\ V^2 \left[e^{(-0.47\,\Delta_R + 2.651)} - \left\{ 171.9 + 51.4\ \ln(\Delta_R) \right\} \ln(S_R - 0.06) \right]
\end{aligned}
\tag{5}
$$

where Δ_R is the displacement ratio as defined earlier (displacement of passing ship relative to displacement of moored ship) and where S_R is the beam-to-beam separation ratio given by S_R = (S-(B_p/2)-(B_m/2))/L where B_p and B_m are the beams of the passing and moored vessels respectively. The coefficients C_X, C_Y, and C_M are used to represent the effects of underkeel clearance as

$$
\begin{aligned}
C_X &= e^{0.0955 - 0.6367\ UKCR} \\
C_{Y+} &= e^{0.5157 - 3.438\ UKCR} \\
C_{M-} &= e^{0.343 - 2.288\ UKCR}
\end{aligned}
\tag{6}
$$

UKCR = Underkeel Clearance Ratio = $\dfrac{d - D}{D}$

The coefficients S_F and S_M are scale factors used to convert from model to full scale and are given by

$$
\begin{aligned}
S_F &= 1.5\text{x}10^{-5}\ L \\
S_M &= 59\text{x}10^{-9}\ L
\end{aligned}
\tag{7}
$$

where L is the length of the moored ship in meters.

Flory's equations are somewhat awkward, in that they use mixed units and give results in full-scale units. Thus, the vessel speed, V, must be given in knots at full-scale, while the forces are given in metric tons full scale and the moment is given in metric ton-meters at full scale. For application to the lab data, measured values were scaled up to full scale using a scale ratio of 135, to scale the 5-foot long model vessels up to 675 feet or 206 meters full scale. Figure 19 shows a comparison of measured and predicted values for peak loads.

Results in Figure 19 show measured and predicted values plotted against a line of perfect agreement (at a 1-to-1 slope) and also show trend lines fit through the data points showing the mean relationship between predicted and measured values. Results are also separated for the two displacements or drafts of the passing ship: solid symbols show results for the deeper draft (higher displacement) while open symbols show results for the shallower draft (smaller displacement).

For surge forces (top figure), Flory's method under-predicts the measured loads, with predictions being equal on average to 65% of measured values for the deep draft and to 86% of the measured values for the shallower draft. The maximum error (scatter) is more than 50%.

For sway forces (middle figure), Flory's method under-predicts for the deeper draft, with predictions averaging 74% of measurements, but over-predicts for the shallower draft, with predictions being on average 119% of measured values. Maximum errors are near 100% as several predicted values are near zero despite non-zero measured values. These occur for tests with small D/d ratios where the value of UKCR is greater than unity. The depth corrections of Flory are very small for these conditions and essentially predict near zero loads when, in fact, non-zero loads are measured.

For yaw moments (bottom figure), Flory method predicts well for the deeper draft, with predictions exceeding measurements by just 4% on average. However, scatter is again large and predictions are again in error for deep water conditions as Flory's correction for underkeel clearance is too small. Flory then over-predicts for the shallower draft (smaller displacement) by 99% giving predicted values that are a factor of two larger than measured.

In general, results in Figure 19 indicate that the Flory method is not very reliable for widespread use. It appears to be too sensitive to the displacement ratio and it the corrections for UKCR appear flawed.

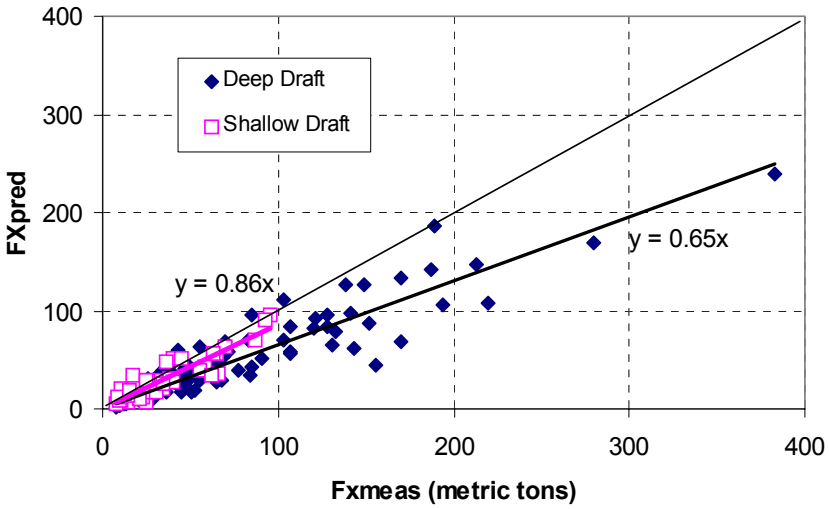

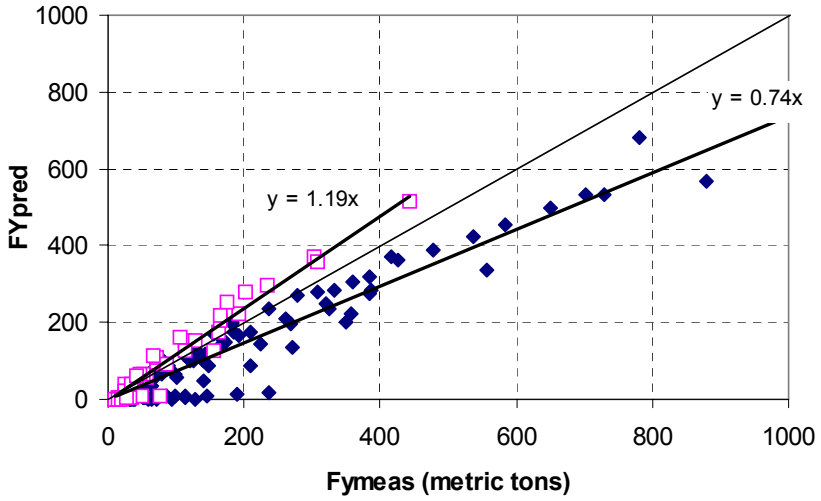

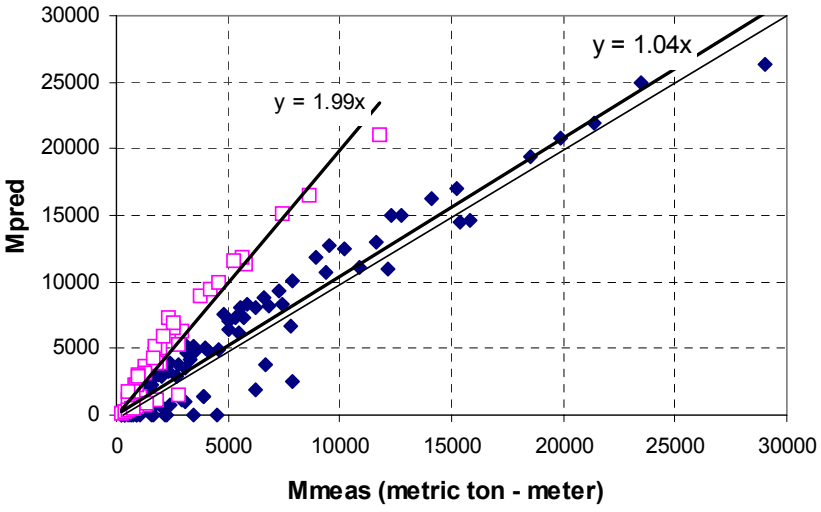

Figure 19. Comparison of measured peak loads to values predicted using Flory method.

Seelig Method in PASS_MOOR

The prediction method adopted in the spreadsheet PASS-MOOR is composed of two parts as described by Seelig (2001). First, deep water predictions are based on the theory of Wang (1975) and account for ship speed, ship dimensions, and separation distance. Second, empirical adjustments are applied that account for effects of reduced underkeel clearance.

The deep water predictions are obtained from dimensionless graphs. An example is shown in Figure 20 for the sway force; similar graphs are given by Wang (1975) and Seelig (2001) for the surge force and yaw moment.

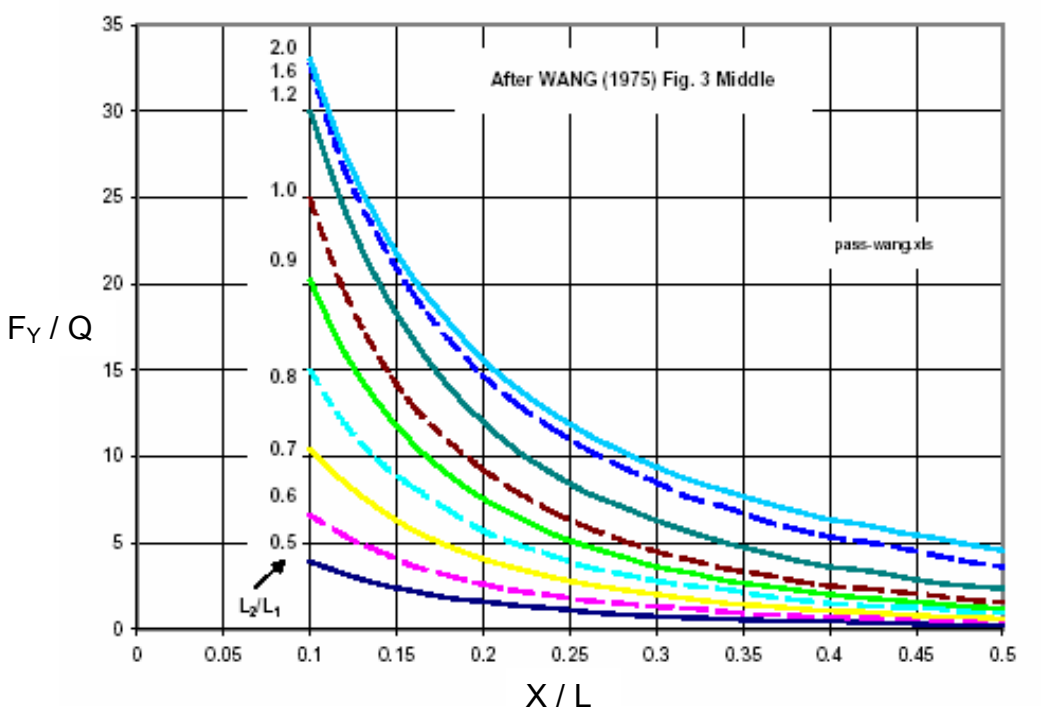

Figure 20. Dimensionless solution for peak sway force in deep water from Wang (1975), reproduced from Seelig (2001). Similar curves are also given for peak surge force and for peak yaw moment (see Wang, 1975 or Seelig, 2001)

The dimensionless graphs give the peak load normalized by a parameter, Q, defined as

$$Q = \rho V^2 L_m^2 \left(\frac{A_m}{L_m^2}\right)\left(\frac{A_p}{L_p^2}\right) \tag{8}$$

where L_m is the length of the moored ship, L_p is the length of the passing ship, and A_m and A_p are the midship section areas of the two ships.

Seelig (2001) then developed correction factors to fit the Wang theory to the data of Remery (1974) and Muga and Fang (1975). Seelig found two types of corrections were required. First, because the Wang theory is for deep water with infinite underkeel clearance, corrections were required to represent shallow water and finite underkeel clearance. Second, Seelig also found that corrections were required for the separation of the two ships. This last correction is problematic because Wang's theory supposedly accounts for ship separation. But Seelig found that additional correction was required when comparing Wang's theory to lab data.

The resulting correction factors developed by Seelig are as follows:

$$
\begin{aligned}
C_X &= 1 + 16\,(D/d)\,e^{(-0.08((G/B)-3.5)^2)} \\
C_Y &= 1 + 25\,(D/B)^{-0.35}\,(D/d)^4\;e^{(-0.08((G/B)-3.3)^2)} \\
C_M &= C_Y
\end{aligned}
\qquad (9)
$$

where G is the beam to beam separation (or gap between vessels), given by G = S–(Bp/2)-(Bm/2) and where subscripts p and m refer to passing and moored vessel respectively.

Figure 21 shows a comparison of measured peak loads to values predicted using the PASS-MOOR spreadsheet. Because Wang's theory, and Seelig's corrections, are given in dimensionless form, they can be readily applied to the lab data in the original model-scale units (V in ft/sec, F in lbs, and M in ft-lbs).

One aspect of PASS-MOOR that is in sharp contrast to the Flory method, is that results are nearly identical in a statistical sense for both the deep draft and shallow draft configurations. Both results produced essentially the same trend line.

For surge force (top figure), PASS-MOOR produces a low degree of scatter but has a bias toward under-prediction, as predicted load is about 66% of the measured load on average. This is nearly the same bias found in the Flory method, but a comparison of Figures 19 and 21 shows that PASS-MOOR has a much smaller scatter. For sway forces (middle figure), similar results are found, as PASS-MOOR tends to underpredict, with an average prediction of about 77% of the measured value. For yaw moments, PASS-MOOR is more accurate and tends to overpredict by just 8% on average.

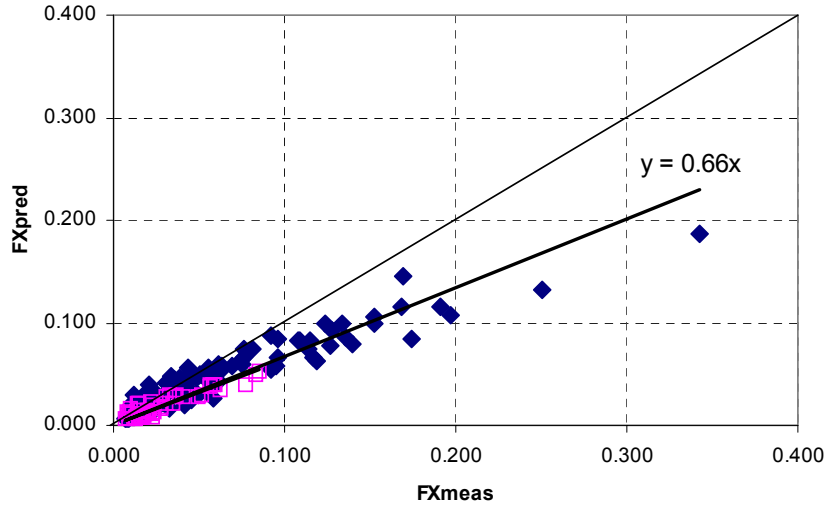

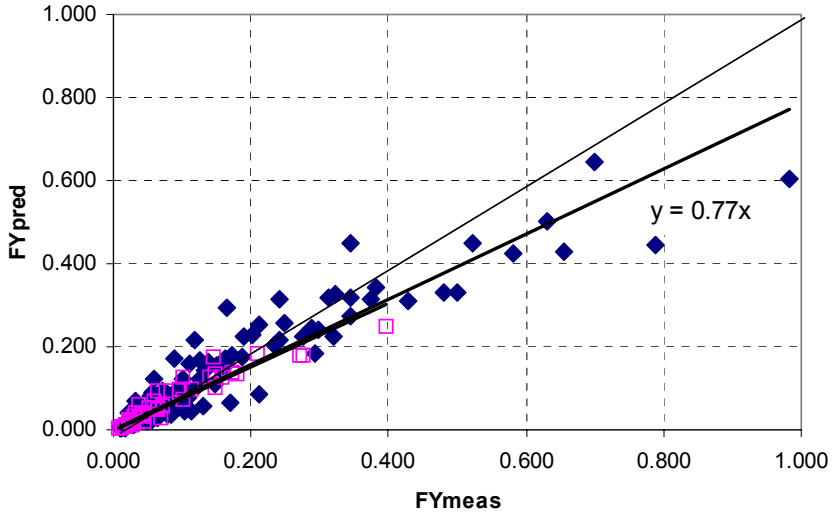

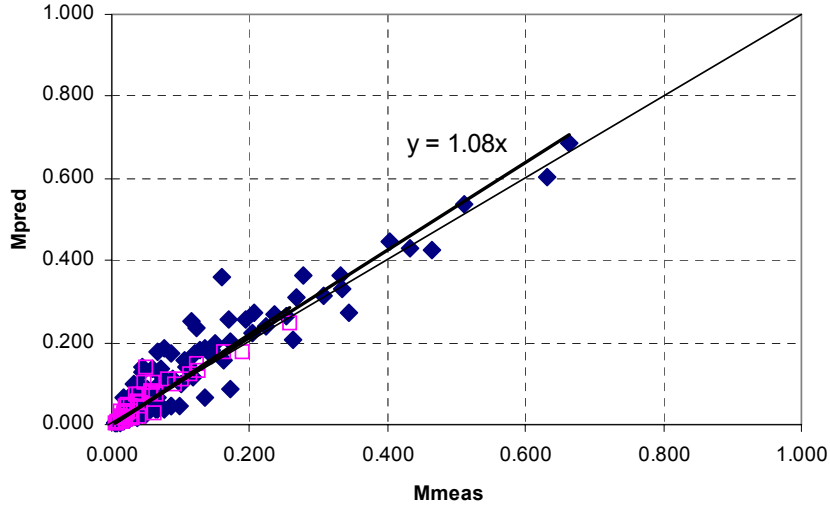

Figure 21. Comparison of measured peak loads to values predicted with PASS-MOOR.

Modification of PASS-MOOR

In order to improve the predictions from PASS-MOOR, the empirical correction factors of Seelig (2001) were re-derived using the data obtained in the present study. The following results were obtained:

$$C_X = 1 + 1.70\, e^{(2.94(D/d))}\, e^{(-0.08((G/B)-3)^2)}$$
$$C_Y = 1 + 0.52\, e^{(4.33(D/d))}\, e^{(-0.08((G/B)-2)^2)} \qquad (10)$$
$$C_M = 1 + 0.48\, e^{(3.87(D/d))}\, e^{(-0.08((G/B)-2)^2)}$$

These are shown graphically in Figure 22. As noted in Equation (4), the experimental results for $\mathbf{F_{x-}}$ and $\mathbf{M_-}$ were slightly higher than the corresponding positive values, so the negative peaks of these parameters and $\mathbf{F_{y+}}$ were used to develop equation (10).

These expressions have the same general form as those by Seelig in equation (9). Several differences are noted however. First, the new correction for surge force is a non-linear function of the draft-to-depth ratio. Seelig had more limited data and adopted a linear relationship as there was insufficient data to adopt any other functional form. The corrections for sway force and yaw moment retain the strong non-linear dependence on (D/d). Second, because PASS-MOOR generally under-predicts the surge and sway force, the new corrections are larger in order to eliminate this bias. Third, while Seelig found the same correction for sway force and yaw moment, the new data suggests less correction is needed for the yaw moment than for sway force.

Predictions carried out using PASS-MOOR with the revised coefficients are shown in Figure 23.

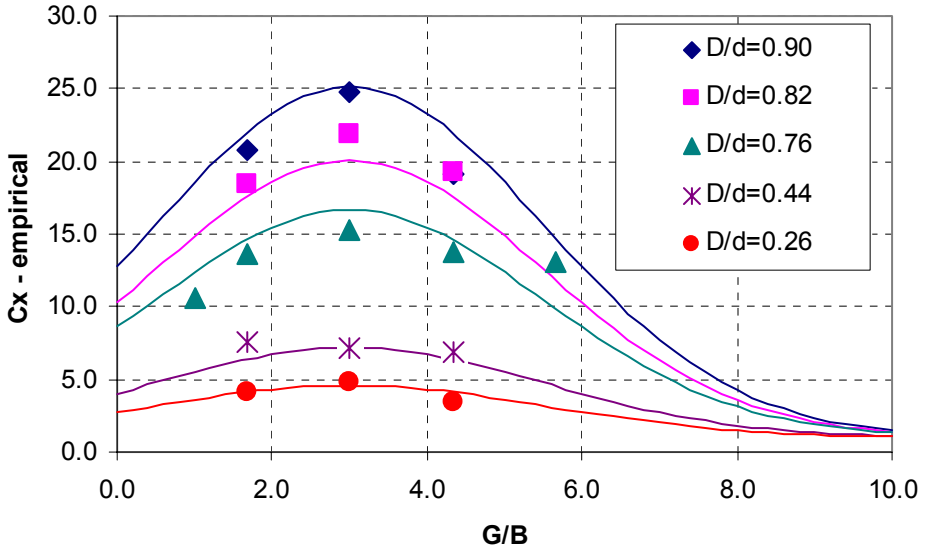

Figure 22a. Surge force correction factor for PASS-MOOR from equation (10)

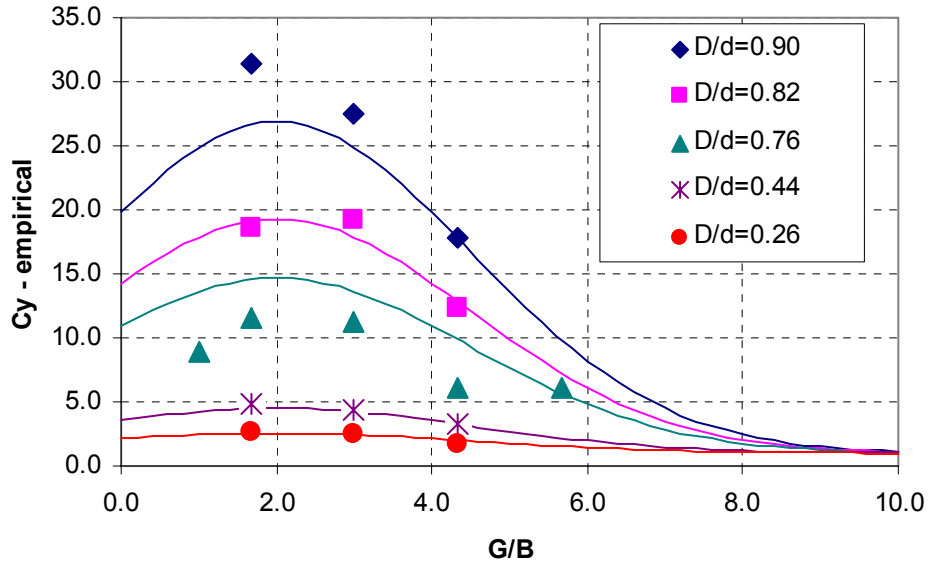

Figure 22b. Sway force correction factor for PASS-MOOR from equation (10)

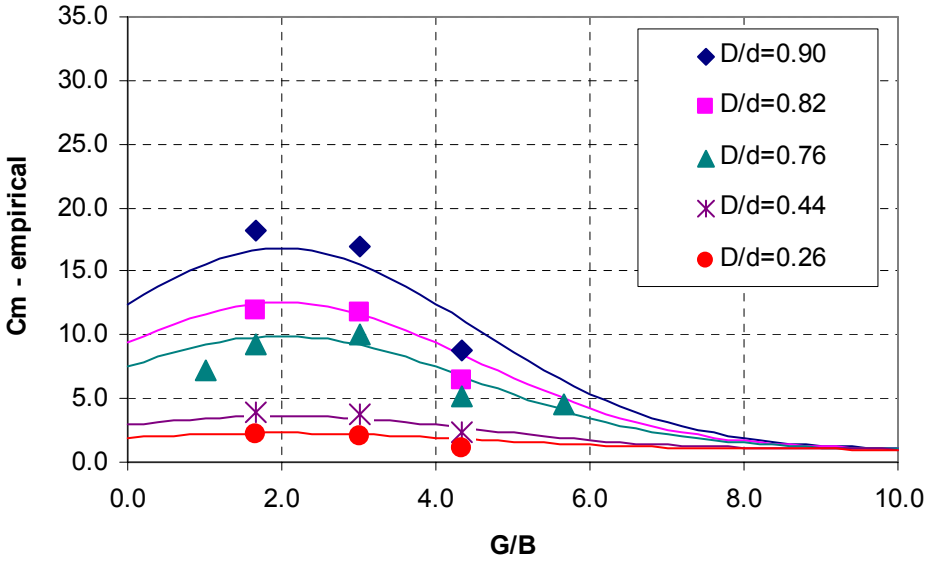

Figure 22c. Yaw moment correction factor for PASS-MOOR from equation (10)

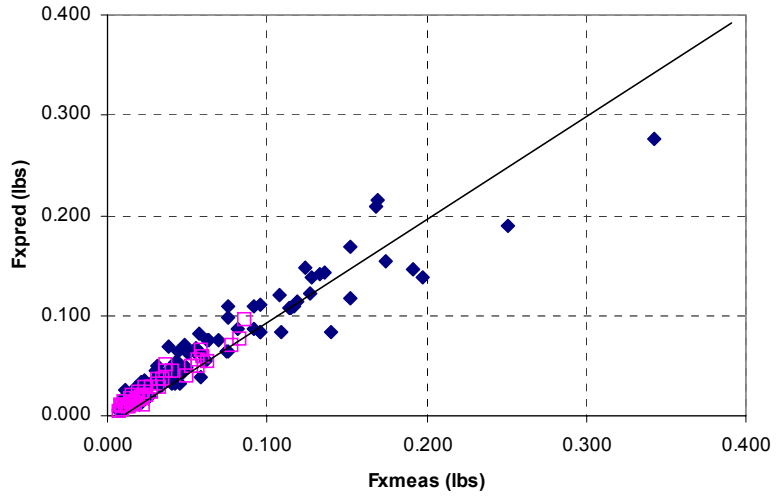

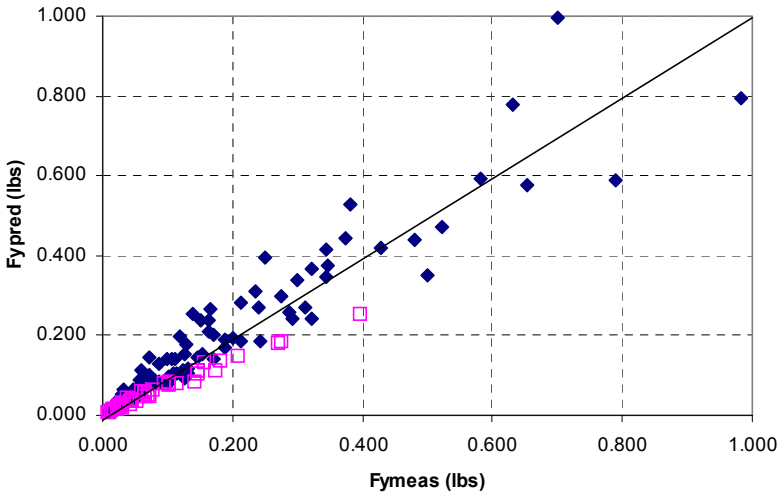

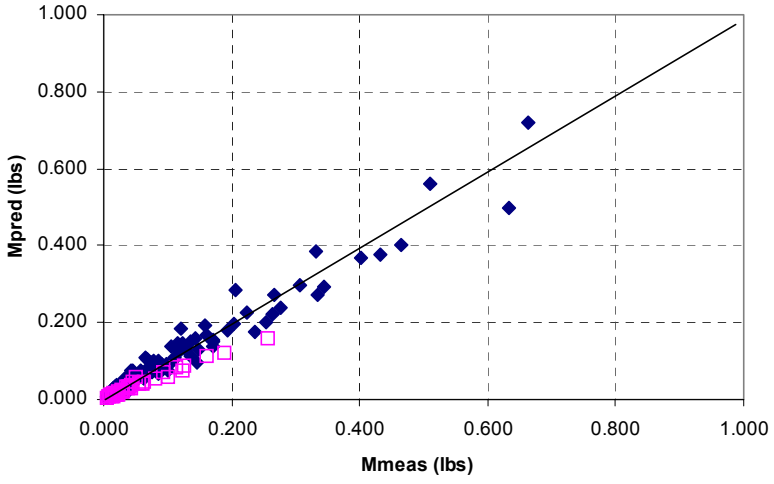

Figure 23. Comparison of measured peak loads to values predicted with PASS-MOOR with revised correction factors in equation (10).

Figure 23 indicates that the revised correction factors in equation (10) result in predicted loads from PASS-MOOR that are in good agreement with measured loads. As expected, there is no bias toward over or under-predicting loads. Scatter is generally comparable to that obtained using the empirical model in Figure 18.

CONCLUSIONS

This study has produced a new set of laboratory scale model data for the loads on a moored ship induced by a passing ship. A total of 144 tests were carried out covering a range of ship speeds, water depths, ship drafts or displacements, and separation distances. Results are for a Series 60 hull form, which is a generic form of commercial vessels that has been widely used in naval architecture laboratories. The degree to which results apply to other hull forms is unknown and additional tests using other hull forms appears needed.

Measured values of peak mooring loads (surge force, sway force, and yaw moment) were first analyzed empirically. A new set of predictive equations was developed to permit simplified estimates of the mooring loads. These equations capture the observed variability in loads with ship separation distance, ship speed, and the draft-t-depth ratio. The simplified equations may be useful for simple hand calculations or for use in spreadsheet predictions.

Measured values were also used to evaluate two of the available methods of predicting mooring loads. The first method, a set of empirical equations by Flory (2002), was found to be unreliable. The formulation in the model for representing the differences in displacement of the passing and moored vessels, and for representing the effect of vessel separation did not accurately reproduce observed variations in loads. The second method, the PASS-MOOR spreadsheet by Seelig (2001), was more consistent in its performance, but under-predicted measured surge and sway forces.

Because PASS-MOOR is used by NAVFAC to predict mooring loads, correction factors used in PASS-MOOR to represent he effects of vessel separation and the draft-to-depth ratio were r e-derived using the new lab data. The revised or re-calibrated PASS-MOOR was then found to provide acceptable predictions of mooring loads.

Despite the large number of tests carried out, additional model tests would prove useful. One lesson learned from the analysis of data is that the mooring loads closely follow a quadratic variation with ship speed. Many tests were carried out with different ship speeds that, in hindsight, were not really needed because of the simple and well-behaved variation of loads with speed. In future tests, it therefore appears that fewer ship speeds should be tested while additional permutations of other parameters should be investigated. These tests used only one hull form, and certainly additional tests should be carried out with additional hull forms. Tests also used only two vessel displacements and this is really insufficient to fully document the variation of loads on a moored ship as vessels having different displacements (or different lengths, beams, and drafts) pass by.

This study has considered a parallel passing configuration and other orientations should be considered. Numerous tests were carried out using a perpendicular configuration, and these will be documented in a subsequent report. This study also considered an open mooring arrangement where the moored ship was surrounded by open water. This was intended to represent ships moored to open piers. Other mooring situations are likely of interest and, in particular, the effect of a closed wharf or quay wall should be tested.

ACKNOWLEDGEMENTS

The author would like to thank Mr. John Zselecsky, Mr. Steve Enzinger, and Mr. William Beaver of the Naval Academy Hydromechanics Laboratory for their assistance with this study. Mr. Enzinger designed and built the original moored ship rig while Mr. Beaver designed and built the new test rig. Mr. Enzinger and Mr. Zselecsky designed and built the towing carriage used in these tests. Mr. Zselecsky also provided considerable assistance with preparation of the ship models and with calibration of the force gages.

REFERENCES

Cohen, S. and Beck, R., 1983, "Experimental and Theoretical Hydrodynamic Forces on a Mathematical Model in Confined Waters," Journal of Ship Research, Vol. 27, No. 2, pp. 75-89.

Flory, J.F., 2002, "The Effect of Passing Ships on Moored Ships," Prevention First 2002 Symposium, California State Lands Commission, Long Beach, CA, September 10-22.

Korsmeyer, F., Lee, C., and Newman, J., 1993, "Computation of Ship Interaction Forces in Restricted waters," Journal of Ship Research, Vol. 37, No. 4, pp. 298-306.

Muga, B. and Fang, S., 1975, "Passing Ship Effects – From Theory and Experiment," Paper OTC 2368, Offshore Technology Conference, Houston, pp. 319-338.

Pinkster, J., 2004, "The Influence of Passing Ships on Ships Moored in Restricted Waters," Paper OTC 16719, Offshore Technology Conference, Houston.

Remery, G., 1974, "Mooring Forces Induced by Passing Ships," Paper OTC 2006, Offshore Technology Conferences, Houston, pp. 349-363.

Seelig, W., 2001, "Passing Ship Effects on Moored Ships," Technical Memorandum TM-6027-OCN, Naval Facilities Engineering Service Center.

Wang, S., 1975, "Dynamic Effects of Ship Passage on Moored Vessels," Journal of the Waterways, Harbors and Coastal Division, American Society of Civil Engineers, pp. 247-258.

Appendix A
Tabulation of Test Conditions and Results

Test Number	Water Depth inches	Passing Draft inches	spacing feet	Speed fps	FX+ lb	FX- lb	FY+ lb	FY- lb	M+ lb	M- lb
1	4.1	3.7	2.0	0.768	0.028	0.041	0.147	0.080	0.070	0.089
2	4.1	3.7	2.0	0.990	0.056	0.045	0.292	0.155	0.136	0.135
3	4.1	3.7	2.0	1.330	0.099	0.119	0.481	0.196	0.273	0.335
4	4.1	3.7	2.0	1.540	0.150	0.174	0.789	0.358	0.572	0.403
5	4.1	3.7	2.0	1.791	0.236	0.168	0.983	0.580	0.743	0.632
6	4.1	3.7	2.0	2.114	0.189	0.476	2.200	0.933	1.550	1.250
7	4.1	3.7	3.0	0.779	0.039	0.033	0.079	0.067	0.054	0.038
8	4.1	3.7	3.0	1.012	0.052	0.049	0.154	0.071	0.078	0.075
9	4.1	3.7	3.0	1.316	0.050	0.058	0.287	0.142	0.134	0.149
10	4.1	3.7	3.0	1.528	0.103	0.117	0.499	0.162	0.279	0.236
11	4.1	3.7	3.0	1.778	0.138	0.136	0.523	0.330	0.430	0.277
12	4.1	3.7	4.0	0.783	0.023	0.023	0.055	0.048	0.030	0.018
13	4.1	3.7	4.0	1.030	0.043	0.047	0.132	0.118	0.044	0.044
14	4.1	3.7	4.0	1.316	0.044	0.049	0.201	0.065	0.082	0.077
15	4.1	3.7	4.0	1.553	0.077	0.076	0.313	0.210	0.153	0.170
16	4.1	3.7	4.0	1.835	0.100	0.128	0.346	0.216	0.244	0.159
17	4.5	3.7	2.0	0.774	0.037	0.042	0.108	0.077	0.055	0.060
18	4.5	3.7	2.0	1.088	0.046	0.059	0.163	0.072	0.097	0.105
19	4.5	3.7	2.0	1.296	0.061	0.092	0.275	0.133	0.150	0.204
20	4.5	3.7	2.0	1.531	0.095	0.127	0.428	0.225	0.242	0.267
21	4.5	3.7	2.0	1.799	0.173	0.152	0.654	0.285	0.371	0.433
22	4.5	3.7	3.0	0.773	0.017	0.023	0.065	0.043	0.031	0.034
23	4.5	3.7	3.0	1.032	0.063	0.058	0.123	0.055	0.054	0.052
24	4.5	3.7	3.0	1.320	0.038	0.055	0.188	0.100	0.069	0.109
25	4.5	3.7	3.0	1.503	0.067	0.096	0.321	0.102	0.122	0.128
26	4.5	3.7	3.0	1.791	0.094	0.108	0.344	0.135	0.202	0.194
27	4.5	3.7	4.0	0.780	0.022	0.024	0.036	0.040	0.018	0.023
28	4.5	3.7	4.0	0.993	0.041	0.046	0.091	0.086	0.026	0.030
29	4.5	3.7	4.0	1.312	0.030	0.061	0.112	0.128	0.040	0.045
30	4.5	3.7	4.0	1.521	0.057	0.069	0.242	0.075	0.075	0.086
31	4.5	3.7	4.0	1.835	0.084	0.096	0.241	0.101	0.117	0.116
32	4.9	3.7	1.5	0.810	0.033	0.040	0.072	0.047	0.038	0.069
33	4.9	3.7	1.5	1.060	0.032	0.039	0.138	0.088	0.073	0.121
34	4.9	3.7	1.5	1.330	0.058	0.076	0.249	0.138	0.129	0.207
35	4.9	3.7	1.5	1.537	0.093	0.124	0.381	0.214	0.258	0.331
36	4.9	3.7	1.5	1.862	0.149	0.169	0.630	0.321	0.389	0.511
37	4.9	3.7	1.5	2.109	0.198	0.343	0.700	0.397	0.347	0.664
38	4.9	3.7	2.0	0.803	0.021	0.021	0.057	0.028	0.026	0.048
39	4.9	3.7	2.0	1.019	0.029	0.031	0.105	0.059	0.061	0.075
40	4.9	3.7	2.0	1.324	0.048	0.063	0.163	0.086	0.093	0.144
41	4.9	3.7	2.0	1.575	0.085	0.114	0.299	0.142	0.181	0.223
42	4.9	3.7	2.0	1.806	0.119	0.133	0.374	0.174	0.213	0.306
43	4.9	3.7	2.0	2.094	0.155	0.251	0.582	0.276	0.333	0.465
44	4.9	3.7	3.0	0.798	0.018	0.014	0.050	0.028	0.026	0.025
45	4.9	3.7	3.0	1.062	0.022	0.024	0.072	0.046	0.043	0.051
46	4.9	3.7	3.0	1.306	0.023	0.042	0.100	0.077	0.044	0.100
47	4.9	3.7	3.0	1.564	0.048	0.064	0.172	0.067	0.083	0.110
48	4.9	3.7	3.0	1.862	0.069	0.115	0.212	0.098	0.100	0.172
49	4.9	3.7	3.0	2.120	0.078	0.197	0.322	0.167	0.148	0.253
50	4.9	3.7	4.0	0.779	0.023	0.020	0.022	0.020	0.016	0.021
51	4.9	3.7	4.0	1.012	0.025	0.020	0.033	0.032	0.020	0.021

52	4.9	3.7	4.0	1.341	0.029	0.032	0.060	0.037	0.022	0.040
53	4.9	3.7	4.0	1.569	0.035	0.056	0.125	0.062	0.039	0.071
54	4.9	3.7	4.0	1.791	0.051	0.082	0.118	0.085	0.052	0.066
55	4.9	3.7	4.0	2.079	0.068	0.152	0.166	0.129	0.093	0.124
56	4.9	3.7	5.0	0.798	0.019	0.020	0.033	0.041	0.017	0.019
57	4.9	3.7	5.0	1.019	0.021	0.026	0.041	0.052	0.025	0.037
58	4.9	3.7	5.0	1.338	0.028	0.040	0.056	0.055	0.034	0.033
59	4.9	3.7	5.0	1.579	0.033	0.039	0.125	0.063	0.051	0.032
60	4.9	3.7	5.0	1.857	0.045	0.076	0.088	0.101	0.057	0.059
61	4.9	3.7	5.0	2.131	0.064	0.140	0.189	0.175	0.080	0.145
62	5.5	3.7	2.0	1.012	0.028	0.029	0.071	0.046	0.030	0.066
63	5.5	3.7	2.0	1.344	0.042	0.050	0.129	0.058	0.073	0.119
64	5.5	3.7	2.0	1.556	0.069	0.096	0.151	0.084	0.093	0.162
65	5.5	3.7	2.0	1.786	0.103	0.092	0.235	0.133	0.111	0.264
66	5.5	3.7	2.0	2.056	0.108	0.191	0.344	0.152	0.195	0.344
67	8.4	3.7	2.0	0.804	0.014	0.017	0.030	0.016	0.021	0.022
68	8.4	3.7	2.0	1.028	0.017	0.026	0.049	0.028	0.039	0.037
69	8.4	3.7	2.0	1.354	0.027	0.034	0.078	0.036	0.062	0.067
70	8.4	3.7	2.0	1.523	0.038	0.040	0.103	0.050	0.085	0.085
71	8.4	3.7	2.0	1.830	0.058	0.075	0.170	0.060	0.120	0.136
72	8.4	3.7	2.0	2.085	0.096	0.109	0.212	0.113	0.173	0.172
73	8.4	3.7	3.0	0.773	0.011	0.012	0.014	0.013	0.013	0.009
74	8.4	3.7	3.0	0.949	0.013	0.013	0.022	0.020	0.017	0.015
75	8.4	3.7	3.0	1.325	0.027	0.018	0.046	0.021	0.030	0.032
76	8.4	3.7	3.0	1.514	0.019	0.023	0.056	0.028	0.042	0.042
77	8.4	3.7	3.0	1.808	0.035	0.034	0.088	0.046	0.055	0.064
78	8.4	3.7	3.0	2.019	0.054	0.061	0.131	0.047	0.081	0.085
79	8.4	3.7	4.0	0.790	0.011	0.012	0.017	0.020	0.006	0.012
80	8.4	3.7	4.0	0.976	0.011	0.015	0.019	0.016	0.009	0.009
81	8.4	3.7	4.0	1.282	0.025	0.017	0.032	0.021	0.015	0.015
82	8.4	3.7	4.0	1.500	0.022	0.023	0.036	0.035	0.024	0.022
83	8.4	3.7	4.0	1.757	0.027	0.036	0.046	0.044	0.031	0.027
84	8.4	3.7	4.0	1.980	0.030	0.043	0.102	0.048	0.036	0.053
85	14.5	3.7	2.0	0.761	0.007	0.008	0.016	0.010	0.011	0.012
86	14.5	3.7	2.0	0.997	0.014	0.013	0.029	0.012	0.019	0.019
87	14.5	3.7	2.0	1.280	0.011	0.023	0.034	0.023	0.032	0.036
88	14.5	3.7	2.0	1.510	0.031	0.026	0.057	0.028	0.043	0.049
89	14.5	3.7	2.0	1.817	0.027	0.039	0.084	0.041	0.069	0.075
90	14.5	3.7	2.0	2.068	0.043	0.045	0.114	0.048	0.090	0.098
91	14.5	3.7	3.0	0.832	0.008	0.009	0.013	0.009	0.007	0.008
92	14.5	3.7	3.0	0.993	0.011	0.011	0.016	0.008	0.009	0.008
93	14.5	3.7	3.0	1.324	0.012	0.015	0.023	0.012	0.017	0.017
94	14.5	3.7	3.0	1.540	0.020	0.016	0.035	0.017	0.020	0.023
95	14.5	3.7	3.0	1.835	0.019	0.019	0.054	0.025	0.034	0.035
96	14.5	3.7	3.0	2.096	0.025	0.031	0.065	0.026	0.043	0.047
97	14.5	3.7	4.0	0.790	0.007	0.007	0.010	0.011	0.003	0.005
98	14.5	3.7	4.0	1.018	0.007	0.008	0.011	0.008	0.006	0.005
99	14.5	3.7	4.0	1.334	0.010	0.010	0.014	0.010	0.009	0.008
100	14.5	3.7	4.0	1.551	0.014	0.011	0.020	0.013	0.012	0.012
101	14.5	3.7	4.0	1.804	0.013	0.012	0.028	0.014	0.016	0.015
102	14.5	3.7	4.0	2.073	0.017	0.021	0.031	0.024	0.021	0.020
103	4.1	1.75	2.0	0.779	0.020	0.018	0.064	0.044	0.040	0.042
104	4.1	1.75	2.0	0.985	0.027	0.028	0.102	0.079	0.078	0.064
105	4.1	1.75	2.0	1.320	0.033	0.036	0.180	0.103	0.117	0.125
106	4.1	1.75	2.0	1.524	0.054	0.078	0.271	0.138	0.187	0.162
107	4.1	1.75	2.0	1.799	0.082	0.086	0.397	0.181	0.287	0.257
108	4.1	1.75	3.0	0.772	0.012	0.017	0.043	0.032	0.018	0.018
109	4.1	1.75	3.0	0.989	0.023	0.024	0.073	0.054	0.040	0.028
110	4.1	1.75	3.0	1.313	0.023	0.035	0.095	0.050	0.055	0.055

111	4.1	1.75	3.0	1.534	0.042	0.052	0.173	0.659	0.090	0.082
112	4.1	1.75	3.0	1.770	0.057	0.058	0.209	0.103	0.140	0.122
113	4.1	1.75	4.0	0.782	0.023	0.023	0.030	0.028	0.019	0.023
114	4.1	1.75	4.0	1.007	0.025	0.021	0.051	0.047	0.019	0.020
115	4.1	1.75	4.0	1.322	0.027	0.031	0.065	0.081	0.030	0.039
116	4.1	1.75	4.0	1.537	0.033	0.036	0.140	0.057	0.046	0.060
117	4.1	1.75	4.0	1.791	0.035	0.059	0.145	0.078	0.095	0.050
118	4.5	1.75	2.0	0.781	0.012	0.015	0.046	0.023	0.029	0.028
119	4.5	1.75	2.0	0.999	0.018	0.020	0.065	0.038	0.041	0.043
120	4.5	1.75	2.0	1.363	0.033	0.040	0.147	0.070	0.080	0.092
121	4.5	1.75	2.0	1.515	0.047	0.063	0.157	0.094	0.114	0.114
122	4.5	1.75	2.0	1.808	0.070	0.083	0.275	0.119	0.176	0.188
123	4.5	1.75	3.0	0.775	0.009	0.012	0.022	0.017	0.012	0.016
124	4.5	1.75	3.0	1.010	0.011	0.023	0.042	0.027	0.024	0.022
125	4.5	1.75	3.0	1.318	0.027	0.023	0.060	0.033	0.037	0.037
126	4.5	1.75	3.0	1.534	0.021	0.049	0.114	0.038	0.060	0.056
127	4.5	1.75	3.0	1.826	0.056	0.056	0.147	0.068	0.092	0.100
128	4.5	1.75	4.0	0.794	0.012	0.013	0.023	0.014	0.008	0.012
129	4.5	1.75	4.0	1.012	0.021	0.019	0.031	0.024	0.013	0.012
130	4.5	1.75	4.0	1.288	0.014	0.028	0.038	0.023	0.017	0.022
131	4.5	1.75	4.0	1.556	0.020	0.031	0.077	0.037	0.029	0.035
132	4.5	1.75	4.0	1.826	0.041	0.056	0.101	0.069	0.053	0.046
133	8.4	1.75	2.0	0.997	0.008	0.013	0.014	0.010	0.016	0.014
134	8.4	1.75	2.0	1.322	0.018	0.016	0.031	0.015	0.028	0.028
135	8.4	1.75	2.0	1.540	0.023	0.015	0.045	0.022	0.040	0.039
136	8.4	1.75	2.0	1.835	0.026	0.032	0.068	0.030	0.058	0.061
137	8.4	1.75	3.0	1.001	0.006	0.009	0.010	0.009	0.009	0.008
138	8.4	1.75	3.0	1.311	0.012	0.011	0.018	0.012	0.014	0.016
139	8.4	1.75	3.0	1.534	0.013	0.010	0.027	0.016	0.019	0.020
140	8.4	1.75	3.0	1.839	0.016	0.022	0.029	0.028	0.028	0.030
141	8.4	1.75	4.0	0.993	0.006	0.007	0.008	0.011	0.005	0.005
142	8.4	1.75	4.0	1.304	0.008	0.009	0.013	0.013	0.007	0.007
143	8.4	1.75	4.0	1.479	0.010	0.008	0.017	0.012	0.010	0.011
144	8.4	1.75	4.0	1.835	0.011	0.014	0.025	0.016	0.014	0.016